THESIS

USING PROTOTYPICAL SITES TO MODEL METHANE EMISSIONS IN COLORADO'S DENVER-JULESBURG BASIN USING MECHANISTIC EMISSIONS ESTIMATION TOOL

Submitted by

Winrose A. Mollel

Department of Mechanical Engineering

In partial fulfillment of the requirements

For the Degree of Master of Science

Colorado State University

Fort Collins, Colorado

Summer 2023

Master's Committee:

Advisor: Daniel B. Olsen
Co-Advisor: Dan Zimmerle

Dan Baker
Jason Quinn

ABSTRACT

USING PROTOTYPICAL SITES TO MODEL METHANE EMISSIONS IN COLORADO'S DENVER-JULESBURG BASIN USING MECHANISTIC EMISSIONS ESTIMATION TOOL

The BU methods estimate emissions by considering activity factors and emission factors averages for an extended period for a large area. Some TD methods use ethane-methane ratio to attribute methane emissions from oil and gas facilities. The bottom-up (BU) inventory estimates are often used to drive the attribution of emissions indicated by TD data to different emission source categories. Despite widespread use, recent studies indicate that traditional bottom-up (BU) inventory methods do not adequately capture how variations throughput and failure conditions impact gas composition and rate of emissions. Traditional BU methods typically do not model gas composition, although it differs among different facility configurations and impacts emissions from different equipment within one facility. Since most BU inventories utilize fixed emissions factors, emissions also do not scale due to throughput, which is particularly important for large emitters associated with failure conditions. Mechanistic emissions modeling can be used to address these shortcomings, and make BU modeling more effective. This study illustrates how mechanistic modeling highlight changes in emissions due to variable throughput and equipment pressures and temperatures for the same production routed through same or different production facility designs. The study uses the same mechanistic models to illustrate how frequency of failure modes impacts both gas composition and total emissions. Results indicate mechanistic modeling could explain observed gas composition shift in emitted emissions from production and midstream facilities over time, a key modeling input to improve voluntary and regulatory methane mitigation efforts.

Note

The Mechanistic Air Emissions Simulator (MAES) tool is currently being updated to model basin emissions for key failure conditions; in effect, the results in this current thesis version are preliminary and refer to Mollel et al., in review, for the completed results.

ACKNOWLEDGEMENTS

Words cannot express my gratitude to my supervisor Daniel Zimmerle and my advisor Prof. Daniel B. Olsen for their invaluable patience and feedback. I also could not have undertaken this journey without my defense committee, who generously provided knowledge and expertise.

I am also grateful to my classmates and cohort members, especially my research teammates, for their help, feedback, and moral support.

Lastly, I would be remiss in not mentioning my family and friends. Their belief in me has kept my spirits and motivation high during this process.

DEDICATION

I would like to dedicate this thesis to my sister Macrine Mollel.

TABLE OF CONTENTS

LIST OF TABLES

LIST OF FIGURES

Chapter 1

Introduction

Methane is the second most potent greenhouse gas (GHG) with a Global Warming Potential (GWP) of 25-28 CO_2e for a 100-year period [12]. As a short-lived GHG, there is increasing interest in controlling anthropogenic sources of methane, as a reduction in these emissions could have a substantial climate impact over decadal time scales. Anthropogenic methane is emitted while producing and transporting coal, natural gas, and oil. It is also the result of agricultural operations, principally livestock manure management, and the decay of organic waste in municipal solid waste landfills and wastewater treatment [11].

Methane is the main component of natural gas within the oil and gas (O&G) sector. The natural gas supply chain is often divided into three sectors: upstream, midstream, and downstream [6]. Upstream operations deal with oil and gas exploration, production, and initial separation of production into gas and oil components and wastewater. The midstream operations then transport gas to gas processing plants, where the gas is upgraded to market standards. Additional midstream transmission and storage infrastructure transports that gas to consumers and provides short-term storage. Downstream operations distribute gas to consumers.

This study is part of a larger research program, Colorado Coordinated Campaign (C3), that did an intensive multi-scale methane emissions study from one production basin, the Denver-Julesburg (DJ) basin, in northeastern Colorado. The research program considered emissions from both upstream and midstream operations in the DJ basin. This study focuses specifically on production facility modeling and demonstrates how high-fidelity emission modeling can be utilized to better understand the causes and mitigation of methane emissions.

Production entails extracting hydrocarbons by separating well production liquid hydrocarbons, gas, water, and solids [6]. A production facility is made up of wells and a wellpad. Wells are often remote from the wellpad. A wellpad includes separators, flares, oil storage tanks, water storage tanks, and compressors. Figure 1.1 shows a diagram of a simple production wellpad facility.

Note that this diagram does not represent an actual facility diagram but will be used to describe major processes in a production facility. Equipment A (wellhead), B (first stage separator), C (second stage separator), and D / E (storage tanks) operate at different pressures. As the fluid passes through these stages, the pressure progressively decreases. When the pressure drops, lighter hydrocarbons rapidly transition out of liquid hydrocarbons to the vapor phase in a process called flashing. The amount of hydrocarbons of different molecular weights flashed at any stage depends on the pressure drop. Therefore, the gas composition will be different for different pressure drops.

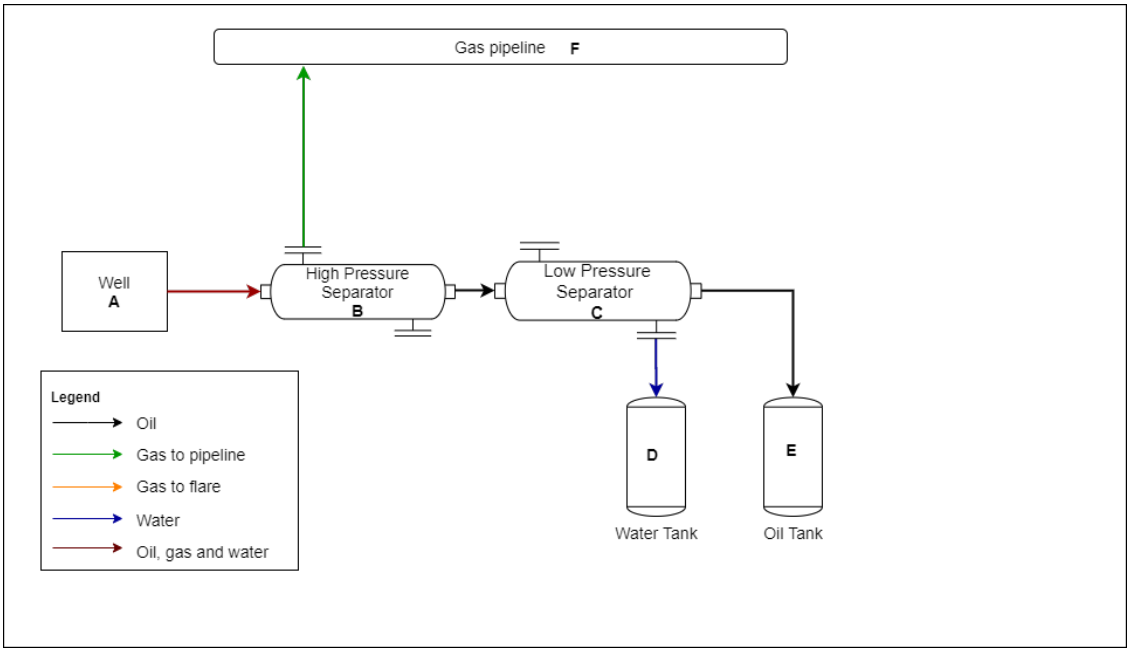

Figure 1.1: A diagram to represent a simple production facility. Mixed gas and liquid from A go through a first stage of separation in B, where most lighter hydrocarbon gas is separated from liquids. The gas goes to F and the liquids go through the second stage of separation at C, where the liquid is separated into gas, water, and oil. In this facility, oil is routed to E and water to D, both of which are atmospheric tanks with internal pressures at or slightly above ambient pressure. Pressure settings for each stage of separation are determined by the facility design and well production characteristics.

Production facilities also have pneumatic controllers, devices driven by pressurized gas or air, used as liquid-level controllers, pressure regulators, and valve controllers. Equipment B and C include liquid level controllers, pressure regulators, and valve controllers.

Other production facility equipment not shown in the figure include vapor recovery towers (VRTs), Vapor recovery units (VRUs), and lease automatic custody transfer (LACT) units. A VRT often acts as a third stage of separation and is normally connected between separators and tanks. Relatively long residence time in the VRT helps reduce volatile organic compound (VOC) emissions from the atmospheric tanks. VRU is a compressor for increasing gas pressure [21] from low pressure equipment to higher gas gathering line pressures. In the diagram above, a VRU could be connected to a low-pressure (LP) separator (C) to increase the pressure of the gas to the gas pipeline (F) pressure. LACT measures liquid hydrocarbons' net volume and composition and then transfers the produced oil to a liquids pipeline [21]. LACTs replace truck loadout from facilities with atmospheric tanks (i.e. oil tank (E) on the diagram above), but are implemented only in regions where an oil pipeline is near the facility.

The C3 study compared methane emissions estimates from traditional bottom-up (BU) inventories submitted to the Colorado Department of Public Health and Environment (CDPHE), aerial top-down (TD) estimates of emissions from two different TD methods, and emissions simulated using Mechanistic Air Emissions Simulator (MAES).

Traditional BU inventory methods calculate emissions by multiplying an emission factor and an activity factor for each known source. BU inventories are commonly used by GHG reporting agents such as by US Greenhouse Gas Inventory and CDPHE Annual Oil and Natural Gas Emissions Inventory Reports [19]. In their simplest form, BU methods do not include variability in emission or activity factors, although more advanced methods include uncertainty estimates for both emissions and activity. For example, emission inventories submitted to CDPHE utilize basic, single-value, emissions factors multiplied by counts of components or process activity. In contrast with regulatory reporting, scientific studies typically use extended BU methods that include probability distributions to represent the variability and uncertainty in emission factors, and often also in activity factors [22].

Since traditional BU methods utilize emission and activity factors collected previously, generally in publicized field campaigns, calculated emissions are averages for a large population of

facilities over an extended period. This presents several problems associated with traditional BU inventories: lack of variability in emissions, emissions do not scale with the size or throughput of facilities, and a lack of temporal and spatial resolution that reflect the significant variation in emissions over time [3, 20, 22].

Methane emissions have also been estimated using TD methods [10, 20]. In some TD methods, measurements occur during short periods by observing individual plumes at facilities [10], while other techniques perform mass balance at a regional scale using multi-hour observations [15, 17]. Difference in the time scale of TD methods - seconds to a few hours - and BU methods - long-term averages - complicate efforts to compare estimates.

Current TD methods use methane-specific, or are methane-ethane instruments. Since methane is emitted from both biogenic and thermogenic processes, attributing methane flux to specific sources remains challenging. In O&G, methane is typically co-emitted with heavier hydrocarbons and VOCs, and often the ethane-methane (C2/C1) ratio is utilized to attribute methane emissions between O&G and other sources when performing regional estimates where methane emissions are a mix of multiple sources. Typically, the BU inventory estimates are used to drive the attribution of emissions from TD data [15, 17]. Since traditional BU methods do not model the gas composition for specific facilities, TD methods often assume a simple universal gas composition, such as assuming that the basin C2/C1 ratio from all O&G operations is the same as the C2/C1 ratio from wellhead production. However, as noted above, and typically not modeled in traditional BU methods, gas composition varies dramatically between facilities, stages of separation on production facilities, and the location of emissions from equipment. As a result, aggregate emissions C2/C1 ratio may differ substantially from the production C2/C1 ratio.

A common TD method is aerial plume imaging, which measures methane emissions from concentrated sources, also known as 'point source' emitters. All current aerial imaging solutions use methane-specific instruments. Therefore, co-emitted volatile organic compounds (VOCs) are not characterized. Typical aerial plume methods estimate emissions from brief observations (seconds) of many facilities with little knowledge of the facility's operational state. For example, published

results from these methods generally do not distinguish maintenance emissions from fugitive emissions. Maintenance may represent a large fraction of total emissions during mid-day when there is sufficient light to image plumes. Maintenance emissions such as manual liquid unloading (blowing liquids from well bore) and blowdowns (depressurization of equipment) produce high emissions over a short period and are usually initiated by operators as needed [20]. Combining daytime maintenance emissions with unplanned fugitive emissions may misstate total basin emissions.

Past studies have identified systematic differences between TD and BU estimates of basin-scale emissions [15]. TD estimates are usually larger than BU estimates. One likely reason for low BU estimates is inaccurate emissions factors due to the under-representation of large emitters. Additionally, natural gas emissions vary temporally and spatially therefore the averaged emission factors often differ from emissions occurring at a shorter period of time [20].

MAES was developed to address the three problems identified above, i.e., large emitters due to failure conditions, gas composition at different process stages at a facility, and variability in emissions due to variability in facility throughput. MAES is a new approach to the BU inventory method that includes both temporal and spatial variability. MAES models emissions to a one-second granularity with each emission event associated with geospatial coordinates. Additionally, it uses Monte Carlo (MC) methods to propagate uncertainty and variability from inputs to calculated emissions [4, 22].

MAES addresses the variability in emissions by using mechanistic modeling of major equipment units to tie emissions behavior to the combination of the fluids (liquid and vapor) flowing through the equipment and the operational state of the equipment, including key failure modes. Unlike physical modeling, which simulates the pressures, temperatures, and other physical parameters to understand fluid flows through equipment, mechanistic modeling ties all emissions behavior to the fluids traveling through the equipment and the state of the equipment, including failure states of principal components on the equipment unit. The simplification from physical to mechanistic modeling accelerates computations, allowing MAES to simulate long duration - 100s of years is common - to capture rare emission behaviors from complex facilities.

Simulating a facility in MAES with and without a failure model, or with varying throughput, supports sensitivity analysis for emissions driven by the frequency and severity of a failure condition. The following example illustrates how MAES addresses large emitters caused by failures of key components on equipment. Referring to Figure 1.1, separators have dump valves. Controllers driving these valves utilize a float in the tank to sense fluid level, then open periodically to control the liquid level in the separator. In proper operation, the controller and dump valve drain the fluid without allowing the gas to escape through the valve. A typical failure mode in a separator is a 'stuck dump valve,' where the valve does not close entirely due to the build-up of deposits, a control failure, or corrosion. In this case, high-pressure gas will escape downstream from C to D and/or E, substantially increasing the gas volume in D and E. Since the atmospheric tanks are rated for low pressures, pressure relief valve (PRV) on the tanks will open to vent the gas in the tanks (D and E) to the atmosphere.

MAES simulates the gas flow into the tanks by modeling the frequency (probability) of a separator dump valve being stuck open and the observed fraction of gas lost through the valves when partially open. Over-pressure in the tank is modeled by setting limits to the volume of gas that can be vented through tank vent piping, after which the PRV opens to vent to the atmosphere. MAES uses this fluid flow parameter to replace a complex physical model with well-understood mechanistic settings that support fast, realistic simulation of complex physical behavior. For example, if wells cycle on/off – a common method of increasing oil production from wells – varying well fluid flows will travel through the facility model, driving varying gas loss from separators and varying atmospheric emissions from the tanks. As a result, the MAES BU model estimates not only the long-term average emissions but also the variability in emissions minute-to-minute.

MAES attacks the gas composition problem by calculating gas compositions for each unit where data is available. For example, at well pads, gas composition depends on wellhead fluid composition, pressure at each stage of separation, and process temperature [8]. Changing equipment configuration and simulating in MAES shows the effect of configuration changes on total emissions and the gas composition of emissions.

For this study, gas composition at well pad (production) facilities is of primary interest. The production strata tapped by the well determine wellhead fluid composition, which in turn impacts the production strategy. Unfortunately, wellhead fluid composition is difficult to measure directly, and few estimates are publicly available. To estimate wellhead composition, this study uses a thermodynamic searchable database developed by the University of Texas, Austin, which uses commonly available parameters, such as facility gas-to-oil ratio, API gravity, process temperature, etc. to estimate wellhead fluid composition; see Cardoso-Saldaña et al. [8] for additional details.

After estimating the wellhead fluid composition, the instantaneous flash volume and gas composition at each stage of separation is computed from flash gas computations (Peng Robinson Equations of State and Henry's Law) [7]. Flash gas is the vapor produced from the depressurization or heating of an oil mixture during different stages of production. There are two types of flash gas: instantaneous flash and working flash. Instantaneous flash is the spontaneous vapor produced from depressurization. In contrast, the working flash is produced when liquid is held for long periods (days), accompanied by (typically cyclic) pressure changes and evaporation. The mass rate of working flash generally is much lower than the instantaneous flash, and working flash vapors contain a larger fraction of heavy hydrocarbons. Currently MAES does not model working flash. Since most methane is separated in instantaneous flash, simulation results for greenhouse gas purposes are not substantially biased by omitting working flash; this would not be the case for modeling VOCs for ozone or aerosol work.

Since equipment B, C, and D in Figure 1.1 operate at different pressure, the gas composition will be different for each equipment piece. MAES models instantaneous flash only. In the case of a stuck dump valve failure model explained above, a stuck dump valve in C will cause flash gas from the separator to be transported downstream to D and E and emitted to the atmosphere. In this case, instead of the gas composition at the tank being a 'rich gas' with a high fraction of heavier hydrocarbons, emissions will be diluted by a much large flow of light hydrocarbons (e.g., methane) bypassing the valve.

Chapter 2

Methodology

The objectives for the modeling in this study are to address the three deficiencies from traditional inventories: gas composition changes, failure conditions, and variability in facility throughput. Additionally, it addresses how to efficiently model the production complexity in a basin, i.e., how to map more than 4000 individual facilities into a set of models that can be simulated within reasonable computational and modeling labor constraints.

2.1 Prototypical Sites

Oil and gas facilities have changed significantly over time in the DJ basin. Most changes in facility design over the last several decades were aimed at either decreasing emissions or increasing production from these facilities.

For example, in the early 2000s, a typical production site in the DJ Basin had one or two stages of separation to separate gas, oil, and water, which were stored in atmospheric tanks on site awaiting collection by periodic truck loadouts. The wells in this era were primarily vertical [21], resulting in sustained production over many years. Some sites had a VRU connected to the lower pressure separator, and others had a flare connected instead [18].

In comparison, more recent production facilities (typically after 2014) have horizontal wells [21], which typically experience rapid decreases in well bore pressures, accompanied by a rapid decrease in production. As a result, shortly after the start of production, most newer facilities are retrofitted with equipment to increase production as well bore pressures decrease, including plunger, gas, or rod lift systems and cycled well operation. Additionally, changes in drilling practice and increasing land-use pressures have resulted in larger, more complex well pads, connected to wells distributed in clusters nearby. The resulting facilities are substantially more complex than those built in the early 2000s. Recently, some companies have implemented production facilities

without atmospheric storage tanks, also called ‘tankless’ facilities, to reduce both emissions and surface footprint [9].

Given changes in production in the last 25 years, the DJ basin, like many other production basins, currently has many vintages of production facilities in operation, ranging from simple single-well facilities with one or two stages of separation to complex well pads with 3 or 4 stages of separation and additional supporting equipment [6].

The MAES model estimates emissions from either a single facility or multiple facilities in a geographic area [22]. Current data indicates the DJ basin has approximately 20,000 actively producing wells and 4,000-5,000 wellpads [1]. The wells and wellpads in the DJ basin have common features based upon age, company, regulation requirements, etc. Discussion with the partner operators developed an evolution of DJ basin production facility designs, which differ between operators and date when the facility wa constructed, as shown in Table 2.1. There is sufficient similarity between a sufficiently large population of production facilities in the DJ basin, to identify common simulation prototypes applicable to multiple facilities [21].

Table 2.1: The evolution of production facility designs in the DJ basin from three C3 project partner operators

Year	Facility Designs
Company A	
Early 2000	Vertical Wells
	1 separator per well
	Standard 3 phase separator
	1 stage of separation
2012-2014	Start of horizontal drilling
2017-2020	Fully horizontal wellpads
	3 stages of separation
Company B	
Pre 2011	Vertical wells
2011-2013	2 stages of separation
2014	Horizontal wells
	2 stages of separation
2020	3 stages of separation
Company C	
Before 2012-2013	Vertical wells
	1 stage of separation
2013-2014	Early horizontal wells
After 2014	2 stages of separation

Through multiple working sessions and data exchanges with partner operators, an extensive effort was made to understand the configuration of sites in the DJ basin. For modeling emissions in MAES, common prototypes representing production facility configurations, called prototypical sites (PSs), were developed. The PSs were categorized according to the number of stages of

separation. For a given number of stages of separation, PSs varied by other major equipment in the site such as type of separator, presence of storage tanks, whether the storage tanks have flares or not, and presence of a VRU. For example, within one PS with a single separation stage, there are facilities with storage tanks and some without storage tanks (tankless facilities), requiring two PSs for this case. The first PS has a single stage of separation with storage tanks, and the other is a single stage of separation directly feeding oil and/or water pipelines – i.e. a tankless facility. This distinction is vital since tankless facilities often have lower emissions than a facility with a tank [9]. According to Lyon et al., over 90% of detected emissions from a production facility are from tank vents and hatches; therefore, eliminating tanks significantly reduces emissions from a production facility [14].

In total, 13 PSs were developed. Figure 2.1 shows all 13 in a decision tree format for classification (see Section A for a detailed description of all PSs). Developing prototypical sites is an ongoing process as PS models are used in modeling and partners match their facilities in the DJ basin with the PSs.

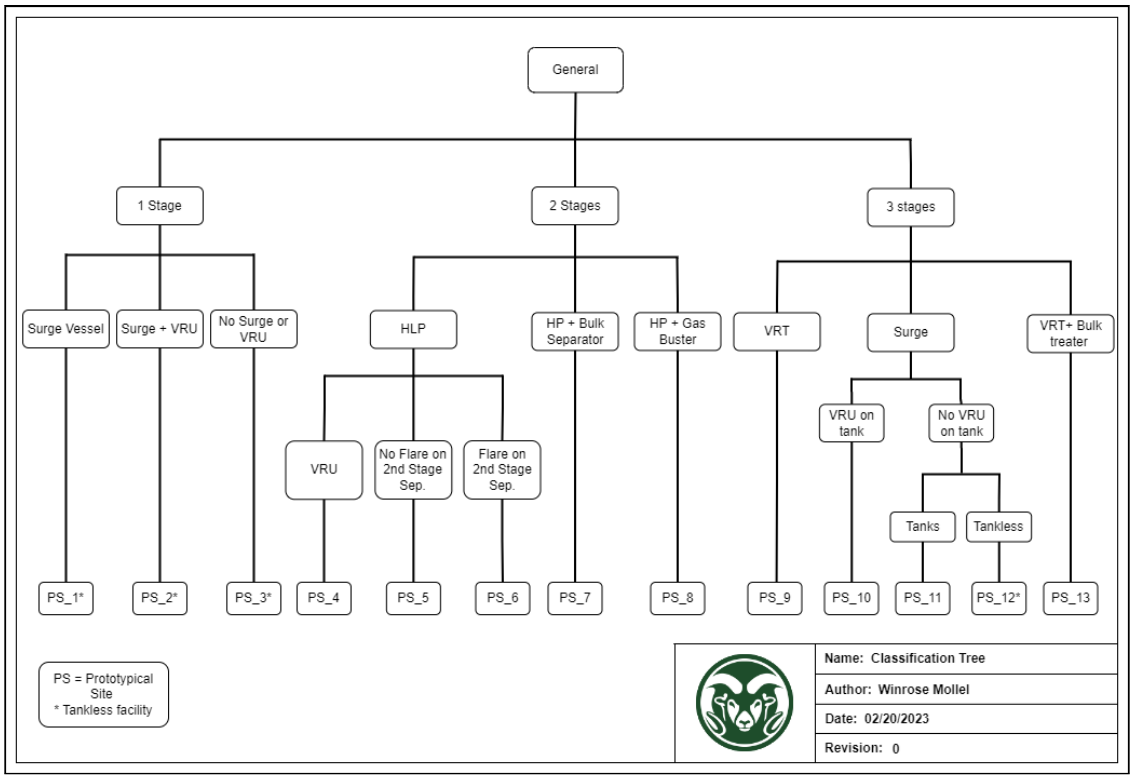

Figure 2.1: A decision tree representing the 13 developed prototypical sites in the DJ basin. The sites are categorized by the stages of separation and major equipment present in the facility. There are three PSs with a single stage of separation. These facilities are distinguished from each other depending on the presence or absence of either surge vessels and/or VRUs. There are five PSs with two stages of separation. These sites are distinguished by the type of separators such as a single high-low-pressure combined separator (HLP) or a combination of a high-pressure (HP) separator with either a gas buster or a bulk separator. Sites with a HLP separator are further categorized depending on other major equipment (flare or VRU connected to the LP side of an HLP separator. There are also five PSs under three stages of separation. In these sites, for the first two stages, an HLP or any combination of an HP and a LP separator can be used; the distinguishing factor is what is connected to the third stage of separation.

Once an actual facility is matched with a PS, information on equipment counts and operating conditions, such as separator pressure, is obtained from either a partner operator or relevant inventories. The equipment parameters needed to run MAES are then added to a spreadsheet hereafter referred to as a study sheet. The study sheet also has parameters to specify failure modes and the corresponding failure rates. The study sheet, gas composition files, and emission factors files specifying emission factors for all equipment are inputs for the MAES simulator. Data for all parameters needed to run MAES, such as emission factors, well production, equipment counts,

and operating conditions are obtained from public data sources, published research studies, and partner operators in the DJ basin [1, 5, 16, 23]. Three sample facilities from matched prototypical sites were selected for this study to demonstrate how MAES solves the deficiencies of traditional inventory methods.

2.2 MAES

MAES utilizes two types of models:

- *Mechanistic models:* This type of model is utilized for significant failure conditions where emissions are a function of the fluids traveling through the equipment, or in cases where emissions from one sources should be temporally aligned to emissions from another source. Specific models are described in the next section.

- *Traditional methods:* This type of model uses activity counts multiplied by emissions distributions to estimate emissions in a given facility. To provide the temporal characteristics of these emitters, leak probability and duration utilizes estimates of mean time before failure (MTBF) and mean time to repair (MTTR), see reference [22]

Key emitter types and behavior are described below; a more complete description of the MAES model is available in Zimmerle et al. [22].

2.2.1 Failure Modes

Simulating failure modes is critical for an accurate estimate of emissions since failure conditions may result in large emitters that may account for more than half of the total emissions in a basin [10, 13]. For this analysis, major equipment failure modes include:

1. Stuck dump valve: When a dump valve is not stuck, all gas is passed to the sales pipeline, and all liquid goes to the next stage. When a dump valve is stuck x% of the gas is passed to the next stage of separation or major equipment unit, (1-x)% of gas is passed to the sales pipeline, and all liquid goes to the next stage. Since downstream equipment typically cannot

handle the excess gas due to the stuck dump valve, these failures typically result in large emissions at downstream tanks or other PRVs.

2. Tank battery vent sticking open without any stimulus from upstream fluid flows: when that happens, the tank stays open until any operations personnel detects it, and any gas flashed in the tank may escape to atmosphere.

3. Tank thief hatch being left open or popping open without any stimulus from upstream fluid flows: when it happens, the tank stays open until detected by operations personnel, and any gas flashed in the tank escapes to atmosphere.

4. Tank battery vent opening due to over pressure in the tank: When gas is delivered from upstream fluid flows above a threshold level, the tank PRV opens to vent gas to atmosphere, and will stay open until incoming gas falls below the threshold. As a result, the PRV opens and closes due to the flow of fluids into the tank and may be highly variable over time.

5. A tank thief hatches opens due to an over-pressure condition in the tank, due to similar conditions as the previous model. Once opened, the thief hatch remains open until detected by operations personnel.

This study will focus on the stuck dump valve failure model.

2.3 Sample Facilities

To demonstrate how the MAES model addresses the three problems identified above, simulations were conducted for three representative models of facilities. These facility models were based on the PSs developed for the DJ basin but were explicitly simplified for this study. The facilities represent an 'older' facility, a 'current' facility, and a state-of-the-art 'future' facility model. The models were designed to illustrate the evolution of production facility design in the DJ basin over the last three decades.

The *old* facility is a wellpad with two stages of separation and atmospheric storage tanks for water and oil (Figure 2.2). A mixture of gas and liquids from the well enters the HP separator.

The pressure in the HP separator is lower than the pressure from the well which will cause the hydrocarbons to be flashed from the mixture and directed to the gas pipeline. Water and oil are also separated, some of the water is drained into the water tank and the remaining water and oil are piped to the second stage of separation.

The second stage pressure is lower than the first stage, causing additional hydrocarbons flashing. All the flashed gas is sent to the flare where it is combusted. Water is drained to the water tanks and the oil is drained to the oil tank. Since both water and oil tanks are at atmospheric pressure, below second stage pressure, hydrocarbons will also be flashed in the tanks. Tank flashing contains a higher proportion of heavier hydrocarbons (C3+) than the first and second stages of separation, as noted earlier. All the flashed gas from the water and oil tanks is sent to the flare to be combusted. The modeled combustion process converts all hydrocarbons into carbon dioxide and water; imperfect combustion, generation of secondary combustion products, etc. is not modeled in this study. A stuck dump valve on the LP separator will direct some LP gas to the tanks. The flare is sized for a finite gas flow rate from the tanks. If gas in the tank exceeds this level, the tank over-pressures, and the excess gas is vented through the tank's PRV. This facility uses natural gas to operate pneumatic controllers.

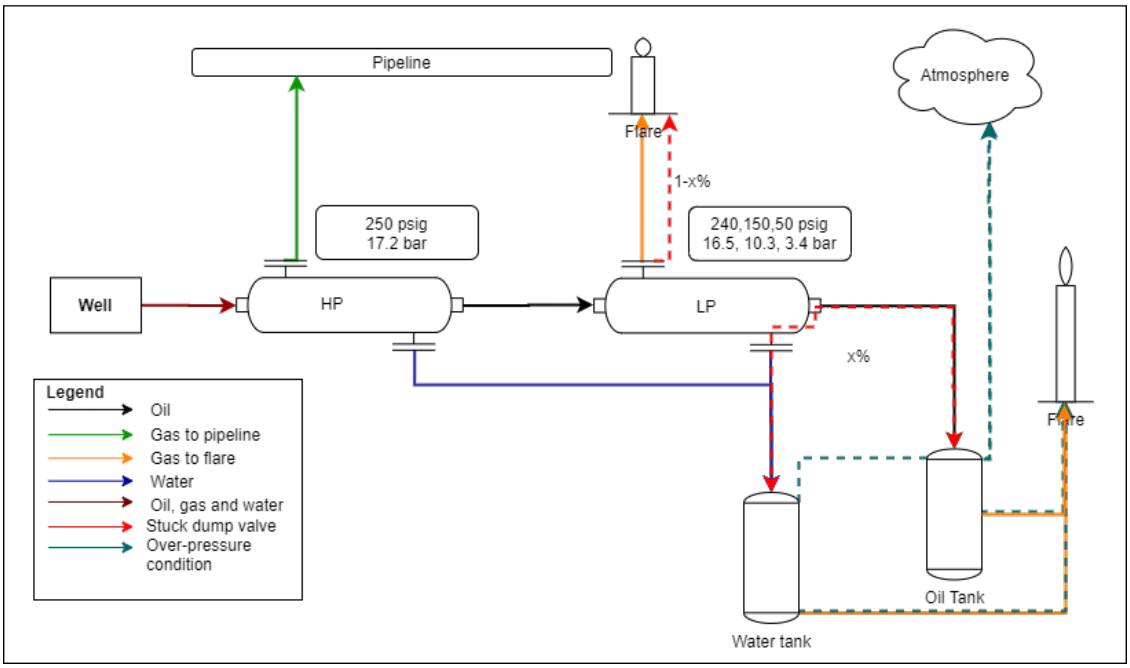

Figure 2.2: Facility diagram representing an old facility with an example of a stuck dump valve failure condition. Values in boxes show the pressure combinations used to generate gas compositions.

The *current* facility is represented by a wellpad with three stages of separation (Figure 2.3) and storage tanks. Gas from the wells follows the same pattern as the old facility, except the flashed hydrocarbons from the second stage of separation are compressed by a VRU to gas pipeline pressure, and the oil is drained to the VRT, providing a third separation stage. For most older facilities of this type, the VRU was driven by a small engine fueled by gas produced on the facility. Newer variants may have electrical service and use motors to drive VRU compressors. The VRT operates at a pressure below that of the second stage but higher than the atmospheric pressure in the tanks; typical pressures are 2-15 psig / 10-100 kPa gauge). Hydrocarbons flashed at the VRT are compressed to the gas pipeline pressure by a VRU, and the oil is drained to an oil tank connected to a control flare. This facility uses air to operate pneumatic controllers.

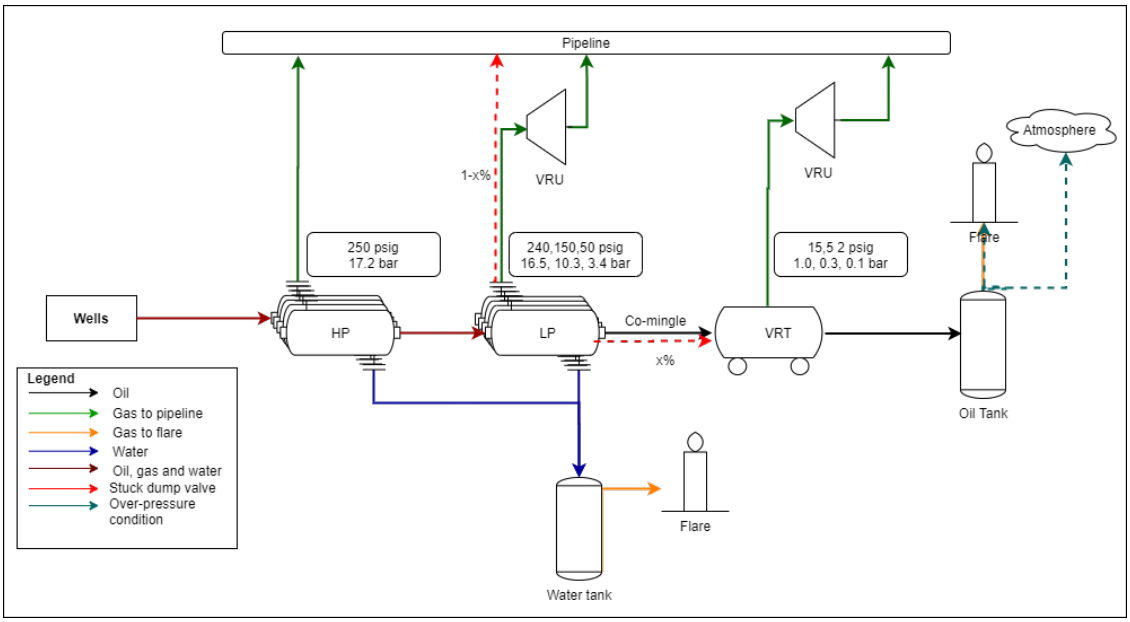

Figure 2.3: Diagram representing a current facility with an example of a stuck dump valve failure condition. The diagram also shows pressure combinations used to generate gas compositions.

A *future* facility is a tankless wellpad with three stages of separation. The flow of the well mixture follows the same separation process as the current site with oil and water routed into pipelines. In general, *tankless* facilities service more wells, and are therefore substantially larger than the *old* or *current* facility configurations. Additionally, most of these facilities are connected to electrical power and utilize electrically-driven compressors for vapor recovery and to provide instrument air for pneumatic controllers.

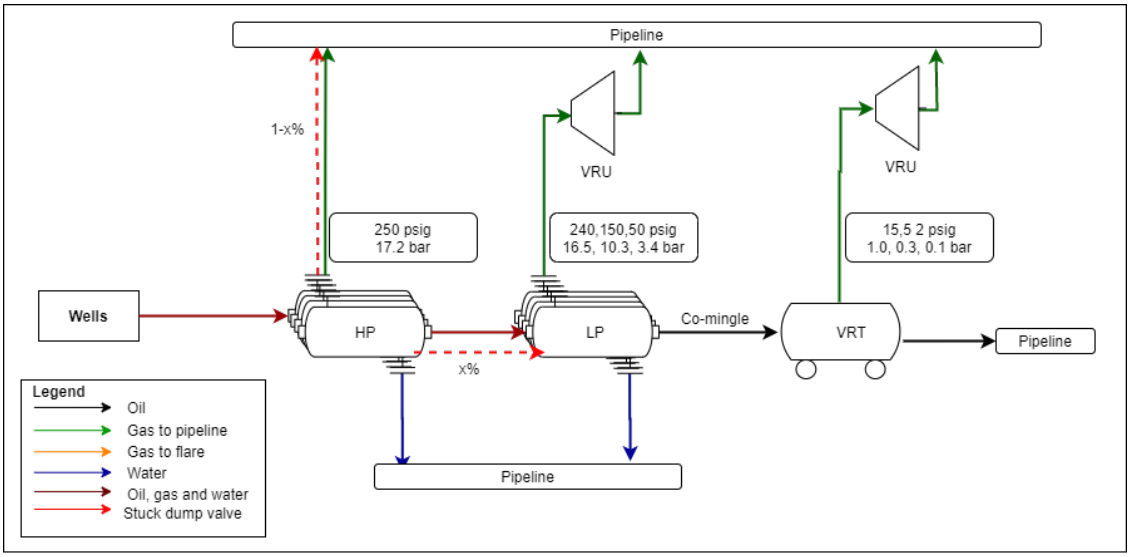

Figure 2.4: Diagram representing a future facility with an example of a stuck dump valve failure condition. The diagram also shows pressure combinations used to generate gas compositions.

Pressures in each stage of separation were varied to examine how changes in gas compositions across each facility impacted the emission rate from the facility, and the gas compositions of emissions. Failure modes rates and throughput were also varied to examine their impact on the facility emissions. Flow of fluids due to stuck dump valve failures are shown in Figures 2.2-2.4). Although field facilities would vary in the number of wells, all facilities where simulated with the same number of wells, baseline failure rate, and baseline production to support inter-comparisons. The simulations were run for 365 days and 100 MC iterations.

Chapter 3

Results

This section uses the three sample facilities in Chapter 2 to show the effects of variability in gas composition, failure modes and throughput on facilities using MAES. This section is divided into three subsections: Gas Composition analysis, Failure modes, and Throughput. The results were presented in box plots. The box is in the inner two quartiles, the whiskers are lines extending above and below each box, and the outliers are observations beyond the whisker length [2].

3.1 Change in Gas Composition

As described in Chapter 1, gas composition depends on wellhead composition, pressure at each stage of separation, and process temperature. For this study, we change only pressure, as the simulations consider the same wells on all facilities and process temperature settings have a secondary impact and are typically kept within a few degrees of those specified in the figures. For old, current, and future facilities, the pressure of the first stage of separation remained constant at 250 psig, the pressure of the second stage of separation varied between 240 psig and 50 psig, and the pressure of the third stage of separation varied between 15 psig and 2 psig; see Table 3.1 for all pressure variations.

Table 3.1: Pressure at different stages of separation for all the old, current, and new facilities in gauge pressure and the pressure ratio in absolute pressure. Total vapor mass in scf per barrel of oil produced at every stage of separation varies with pressure changes.

Stage 1 Pressure (psig)	Stage 2 Pressure (psig)	Stage 3 Pressure (psig)	Pressure Ratio (P1/P2) (-)	Vapor Mass Stage 1 (scf/bbl)	Vapor Mass Stage 2 (scf/bbl)	Vapor Mass Stage 3 (scf/bbl)	Vapor Mass Tank (scf/bbl)
250	240	15	1.04	41,181	3.62	176	28.6
250	150	5	1.61	41,365	42.1	164	9.03
250	50	2	4.09	41,014	114	83.8	4.63

[1] Pressure ratio was calculated using the absolute pressures of both stages of separation

In every major piece of equipment, changing pressure resulted in changing the composition and the amount of the flashed hydrocarbon vapor – which impacts total methane emissions from the facility. Annual methane emissions for each pressure ratio in Table 3.1 for the old, current, and future facilities was estimated using MAES and is shown in Figure 3.1. For the old, current and future facilities, an increase in the pressure ratio correlates with a decrease in methane emissions. According to Lyon et al., over 90% of detected emissions from a production facility are from tank vents and hatches [14]. Referring to Table 3.1, vapor mass in the tank decreases as the pressure ratio increases, explaining the decrease in total methane emission rate from the old and current facilities as pressure ratio increases but not the future facility since it is tankless. As a result of low amount of gas in the tank due to increase in pressure ratio, the amount of gas sent to the flare, which depends on throughput, also decreases, contributing to the overall decrease in facility level methane emissions for the old and current facilities.

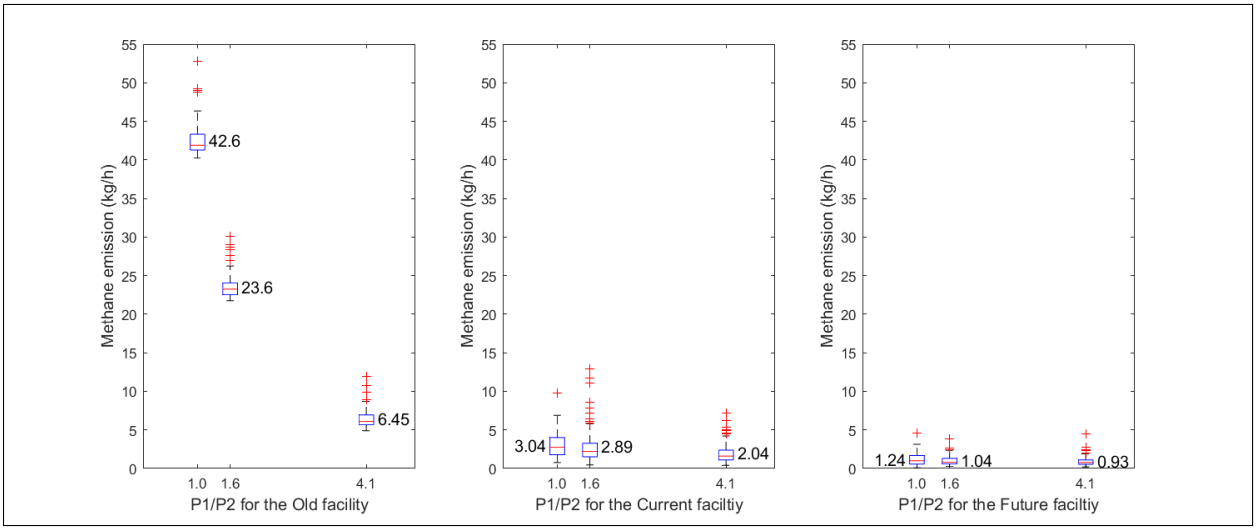

Figure 3.1: From left to right, the impact of pressure ratio variations on methane emissions in the old, current, and future facilities, respectively. As the pressure ratio within the old, current, and future facilities increases, the resulting methane emissions from the site decrease. The number on the box plots shows the annual mean methane emissions.

Overall, the old facility showed the highest methane emission rates, and the future facility showed the lowest methane emission rates for all pressure ratios. The future facility was designed

to minimize emissions by eliminating atmospheric tanks and associated control flares, lowering the corresponding risk from over-pressure events and PRV and thief hatch failures. As a result, major failure conditions that are modeled mechanistically in MAES, have no impact on the future facility, and variations in emission rates are due to random variations between MC runs from non-mechanistic emitters.

As seen in Figure 3.2, emissions from the future facility are emission factor based, i.e from non-mechanistic emitters. The mechanistic emissions from the future facility are from a VRU. The modeled VRU was electric, eliminating exhaust emissions from the VRU, but retaining other compressor emissions [22]. The VRU had blowdowns emissions, which are of a fixed volume and do not change with changes in gas composition. As a result, future facility emissions are predominantly non-mechanistic, for example mechanistic emissions for the pressure ratio of 1 are only 0.000443 percent of total facility emissions. In contrast, both the current and old facilities have atmospheric tanks and flares. For the old and current facilities, gas in the tanks is directed to the flares, and for the old facility, gas from the second stage of separation separator is also directed to the flare. For example, for the current facility, at pressure ratio of 4.1, 4.63 scf/bbl of gas is sent to the flare while for the old facility 118.6 scf/bbl of gas is sent to the flare, resulting in higher emissions from the flare for the old facility than the current facility since the emissions from the flare depend on the amount of fluid passing though it. As a results emissions for the old facilities are predominantly mechanistic while emissions from the current facility are predominantly non-mechanistic. For the old facility, as the pressure ratio increased from 1 to 1.6 to 4.1, the percentage of mechanistic emissions decreased from 93 to 89.4 to 66.5 while for the future facility the percentage of mechanistic emission decreased from 10.2 to 0.859 to 0.535.

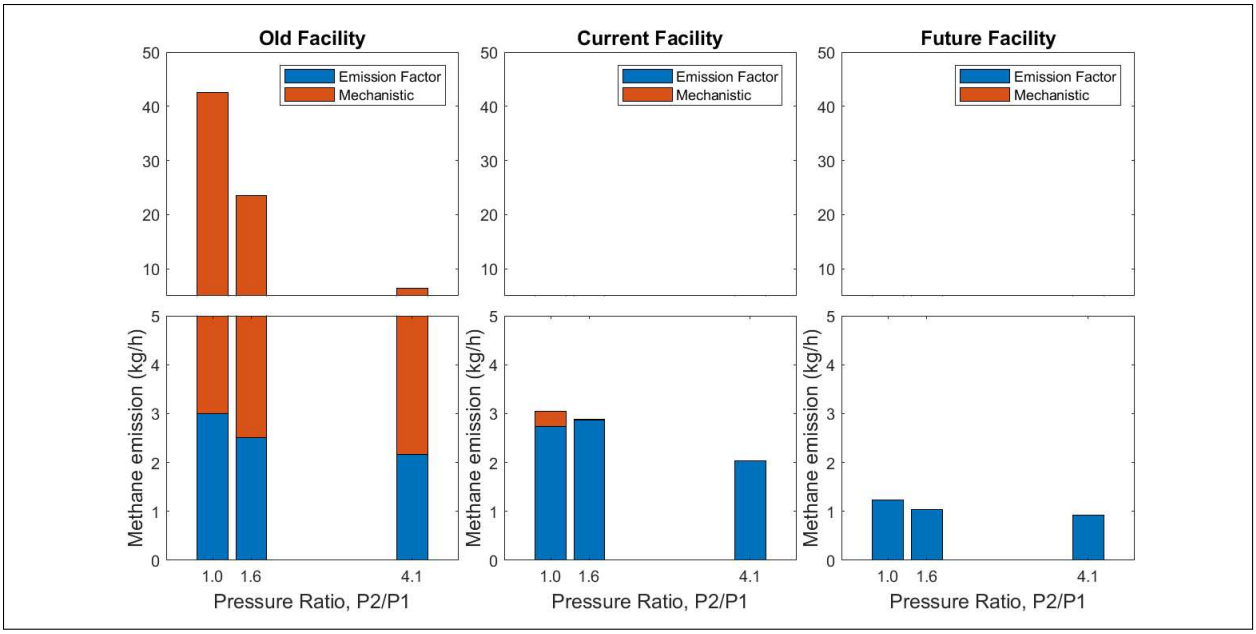

Figure 3.2: methane emission for the old, current, and future facilities categorized into the type of modeling used, i.e mechanistic models or emission factors. For the old, current, and future facilities, increase in pressure ratio correlates with decrease in mechanistic emissions estimates.

Outliers, shown by the red crosses in the Figure 3.1 are observations that lie outside the inter-quartile range times 1.5. MAES estimates emissions using emission and activity factors distributions for non-mechanistic emitters. Emissions estimation for different MC iterations vary depending on the emission and activity factor value used from the distribution. For example, some emitters, such as tank thief hatch and tank vent with probability of leak of about 34.2% and 15.0%, respectively, are driven by emissions distributions that are statistically skewed high (estimated average emission factor of 8.06 and 15.9 scf/s) [23] and when MC iterations draw from the 'tail' of the emissions distribution substantial emissions are modeled. These emitters result in high emissions for MC runs in which they occur and may cause outliers in the MC iteration they occurred.

Equipment that operates mechanistically, such as flares, depend on the amount of gas passing through the equipment. The mechanistic model for flares modifies the destruction efficiency for the flare through three states – operating (98%), malfunctioning - a partial flare failure (90%), and unlit (0%). Flare destruction efficiency is the fraction of gas that leaves the flare partially or fully oxidized. During the operating state, the flare operates normally, and the gas is combusted

at maximum efficiency. During a malfunctioning state, the flare partially operates, and the gas is combusted at less than maximum efficiency. In the unlit state, the gas in the flare is vented into the atmosphere with no combustion. When the flare is unlit, all the gas sent to the flare is emitted into the atmosphere, increasing the emissions emitted in a given MC iteration. As a result, some MC iterations have higher methane emissions than others, which creates outliers in the MC iteration they occurred.

The top ten outliers for the old and current facilities were identified and the MC iteration with the largest outlier was examined. In the MC iteration with the largest outlier for the old facility, "Unflared Gas from Flare", a mechanistic emitter, was the largest emitter contributing about 90.3 percent of the total emissions and was active for 0.414 percent of the entire simulation time. This means all the gas sent to the flare from the tank and the second stage of separation during the unlit state was emitted to the atmosphere. In contrast, in the MC iteration with the largest outlier for the current facility, the largest emitter was "Tank Thief Hatch Leak", a non-mechanistic emitter contributing about 70.2 percent of the total emissions and was active for 100 percent of the entire simulation time.

Using the traditional BU method, methane emissions for each facility would have been the same for all gas compositions since emissions are calculated as a product of emission factors – most often in terms of volumetric whole gas emissions – and activity factors such as the count of thief hatches or tank vents. For example, the approved calculation method for the EPA's Greenhouse Gas Reporting Program (GHGRP) assumes that flare destruction efficiency is uniformly 98%, as most USA jurisdiction classify a drop-off in efficiency as an emissions control failure subject to penalties. The mechanistic modeling approach not only identifies changes emission sources but also varies emissions by both the amount of gas flowing through an equipment unit (e.g. a flare) and performance of that unit.

3.2 Failure Modes

Although in Chapter 2 five failure modes were described, this study chose one failure model, stuck dump valve, to demonstrate that even a single failure mode can have an impact on emissions observed from a facility. For this analysis, we focus on stuck dump valve failure rates for the *current* facility configuration, as there is more data available for stuck dump valves on current facilities [14]. During the stuck dump valve failure mode, the gas that the pipeline should have collected goes to the tank, resulting in over-pressure. The increased emissions from the tank change gas composition of emissions, since the gas passing through the stuck dump valve has a higher methane content. As a result, the C2/C1 ratio of emissions change.

The current site was simulated with and without a stuck dump valve failure mode. When simulating without the stuck dump valve failure mode, the probability of stuck dump valve occurrence was set to happen once every 127 years for each separator. When simulating with a stuck dump valve failure mode, the frequency of the stuck dump valve was set to happen once per year for each separator. The emissions were simulated for 365 days with 100 MC iterations.

To compare with aerial mass balance flights – a form of TD measurement – simulated emissions must be made comparable to air mass sampled by the aircraft downwind of the basin. In the DJ basin, a typical transport time across the basin with prevailing winds is approximately 4 hours. Therefore, to simulate the air mass seen by the aircraft, data are block-averaged to 4-hours. Each MC iteration represents one year for one facility; these emissions were block averaged to four-hour periods, resulting in 2190 emission estimates for each facility. Summing each 4-hour period across the 100 MC iterations provides 2190 time-average emissions for 100 similar facilities. While this facility count is smaller than the DJ basin as a whole, it is sufficiently large to illustrates shifts in both emission rate and C2/C1 ratio.

Figure 3.3 summarizes the C2/C1 ratio change due to changes in failure conditions. The C2/C1 ratio and the methane emissions are four-hour averages across 100 samples representing 100 facilities in the DJ basin. For a case without a stuck dump valve failure mode was 3.17 percent lower than annual methane emissions with a stuck dump valve failure mode. The change is due to the gas

that would have been sent to the gas pipeline from the last (third) stage of separation being sent to the tank instead. The additional gas causes an over-pressure event resulting in more gas emitted to the atmosphere. Since this failure mode can only occur when the stuck dump valve is on the last stage of separation, *and* relatively little gas is flashed off in the third stage (see Table 3.1), there is only a small impact on the total emission rate.

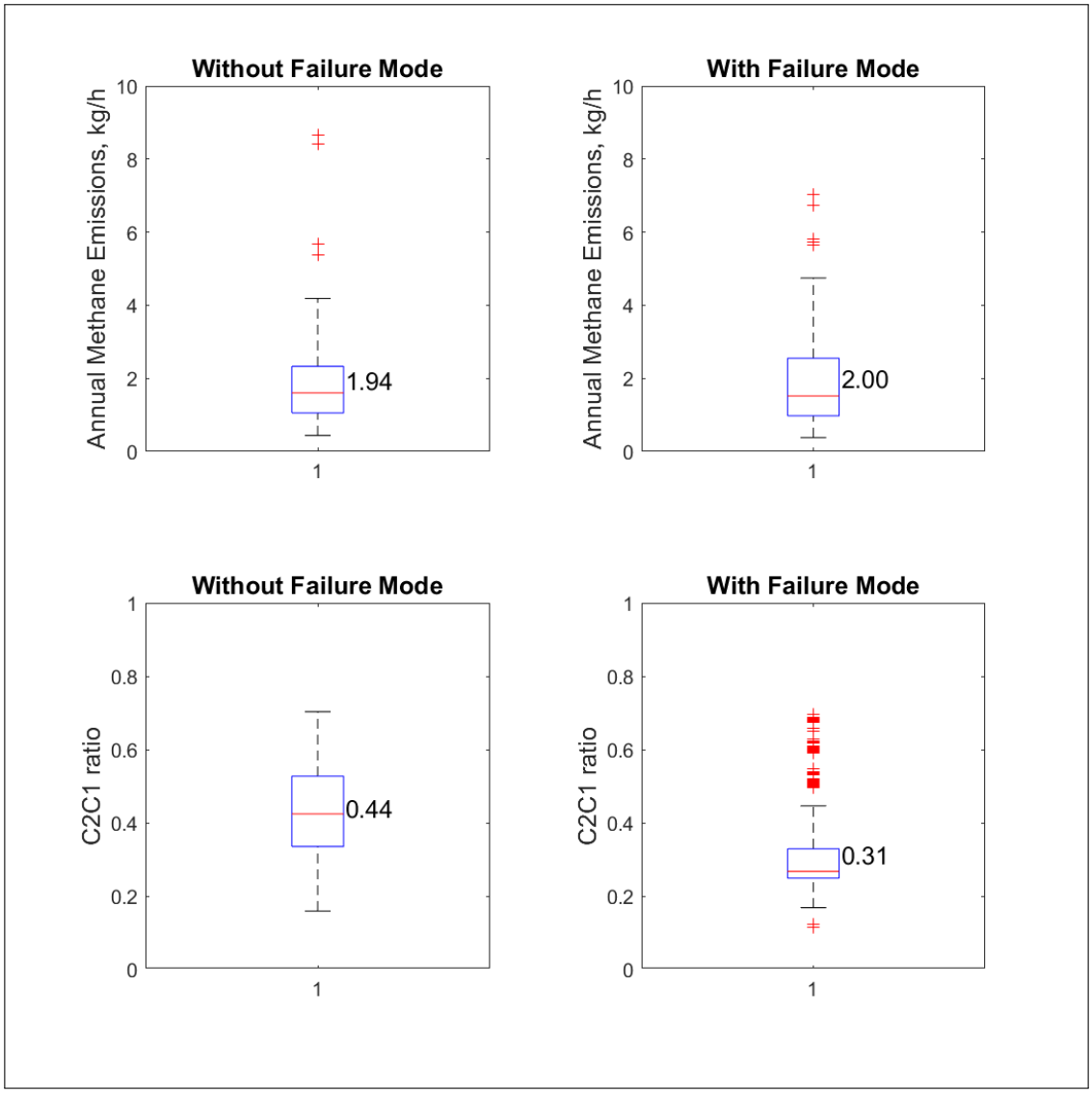

Figure 3.3: The effect of failure modes on the four-hour average C2/C1 ratio. The presence of a stuck dump valve failure condition resulted in a 28.7 percent decrease in C2/C1 ratio, although total methane emitted from the site increased by 3.17 percent as a result of the presence of a stuck dump valve (SDV) failure model

However, the small change in total methane emissions changes C2/C1 ratio substantially. The C2/C1 ratio for a case without a stuck dump failure mode was higher than cases with a stuck dump failure mode because the gas in the tank during a stuck dump valve failure mode has lighter hydrocarbons. As seen in Figure 3.4, the first stage of separation is composed of mainly methane, the second stage of separation has more methane than ethane and the tank has more ethane than methane. During a stuck dump valve failure mode, the gas from the third stage of separation which is rich in methane goes to the tank increasing the amount of methane in the tank and lowering the C2/C1 ratio.

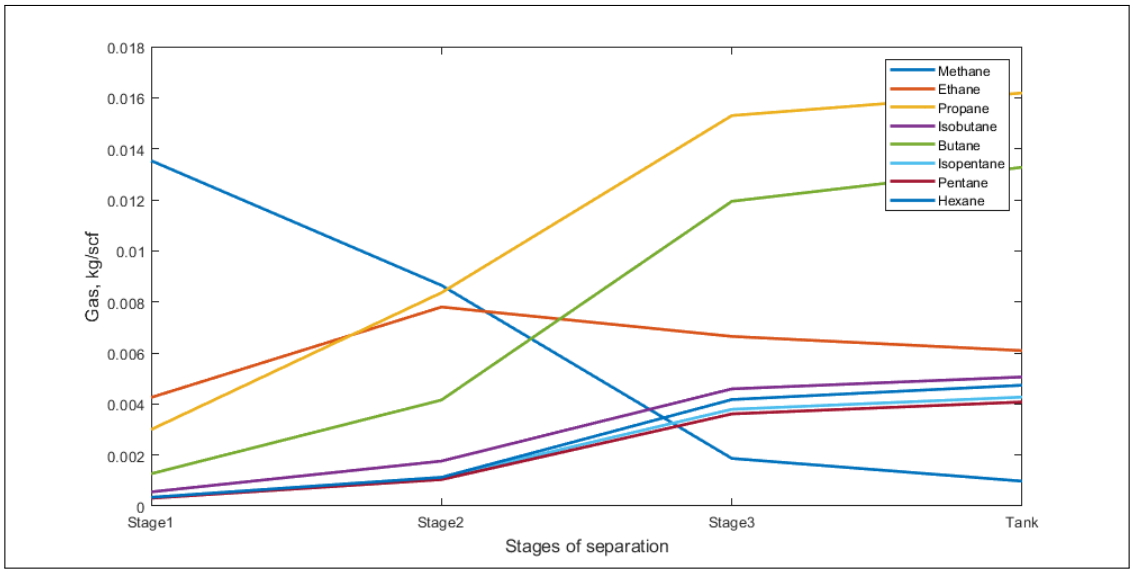

Figure 3.4: The composition of hydrocarbons (HCs) for each stage of separation. Methane decreases as the stages of separation increases while methane increases from the first stage to the second stage, then decreases from the second stage to the tank.

There are more outliers in the case of the stuck dump valve failure model for both annual methane emissions and the C2/C1 – an expected result since a failure model will increase the variability of emissions. During stuck dump valve in a given MC iteration, an over-pressure event occurs and results in higher emissions in the tank than without a stuck dump valve, driving up emissions from the tank and the facility overall. An increase in gas in the tank beyond the amount that the flare can handle will results in an over-pressure event in the tank and the excess gas in the

tank is vented to the atmosphere thus increase in total emissions in the facility. For the current facility, the flare is designed to handle the maximum gas from the tank expected from pressure ratio of 1 in Table 3.1, where the vapor mass gas is 28.6 scf/bbl, all the wells in the facility produce 46.5 barrels of oil per hour, therefore the amount of gas expected to be sent to the flare is around 1,329 scf in an hour. When there is a stuck dump valve in the third stage of separation, a certain fraction of the gas goes to the tank instead of the pipeline, say 50% of the gas from the third stage goes to the tank which is around 4,089 scf per hour. The flare is to handle a finite amount of gas, in this case 1,329 scf per hour, therefore, due to stuck dump valve, flare will handle the maximum amount and the remaining gas in the tank will trigger the PRV to open and emit the the remaining gas to the atmosphere increasing total emissions in the facility.

Figure 3.5 shows an increase in mechanistic emissions from 0.558 percent for a case without stuck dump to 3.54 percent for a case with stuck dump. For the case of stuck dump valve, there were 2 MC runs with an over-pressure event. The MC iteration with largest outlier for the case with stuck dump valve failure mode was identified. In this MC iteration, "Tank Vents Large Emitter" which is the name of the emitter as a result of an over-pressure event, made up 99.7 percent of the emissions and was active for only 0.706 percent of the entire simulation time. This demonstrates that failure models results in large emissions even if the event lasted for a short period and results in change in amount and behavior of emissions.

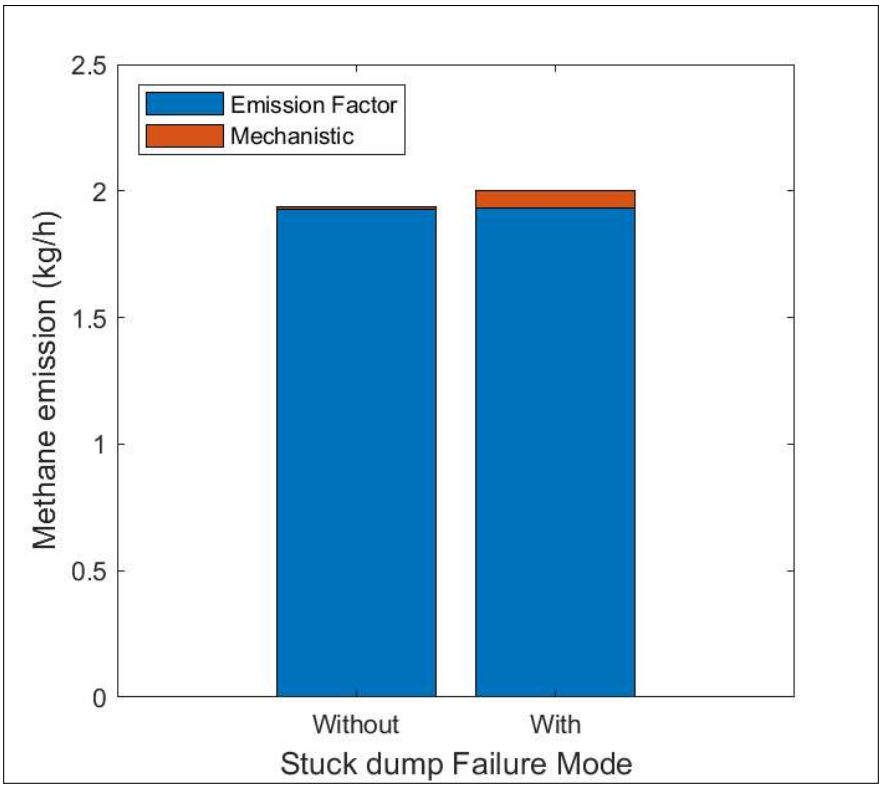

Figure 3.5: Methane emissions by model type used to estimate emissions i.e. mechanistic and emission factors, with and without stuck dump valve failure mode

The C2/C1 ratio is important for TD methane attribution from Oil & Gas sector during TD aerial measurements. MAES can provide insight into the expected C2/C1 ratio, further, it can be used to deduce if a failure was observed during the basin-level measurements.

3.3 Throughput

MAES was also used to show that for the same facility, different throughput displays different emission profiles, which is not the case for the traditional inventory methods. To demonstrate the impacts of varying the throughput on facility methane emissions, well production for all simulated facilities was varied by 0.5, 1, and 2.

As seen in Figure 3.6, an increase in throughput correlates to an increase in methane emissions for the old and current facilities but not the future facility. The future facility was designed to minimize emissions by eliminating atmospheric tanks and associated control flares, lowering

the corresponding risk from over-pressure events and PRV and thief hatch failures. As a result, major failure conditions that are modeled mechanistically in MAES, have no impact on the future facility, and variations in emission rates are due to random variations between MC runs from non-mechanistic emitters. Similarly, while the current facility does not eliminate atmospheric tanks, it has VRUs connected to the second and third stages of separation to compress the gas and send it to the sales line; only the storage tanks have flares for tank vapors. As a result, fewer emissions are directed to flares, and there is less risk of atmospheric emissions due to problems with the flare or equipment upstream of the tank. In contrast, the old facility has a flare connected to the second stage of separation and storage tanks. As seen in Table 3.2, the total amount of gas sent to the flare in the old facility is significantly higher than in the current facility.

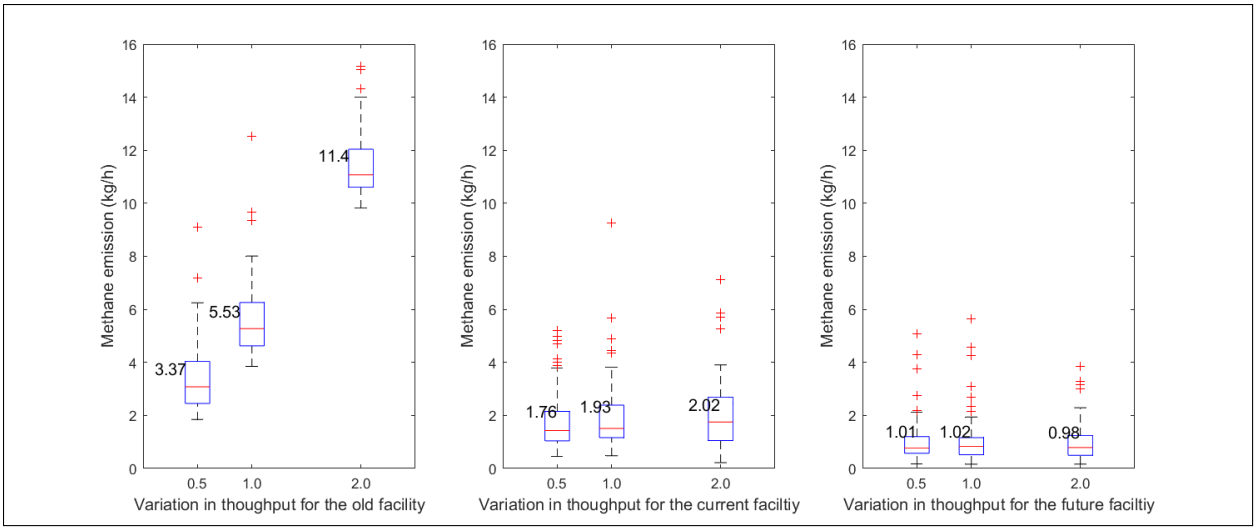

Figure 3.6: From left to right, the effect of changing the throughput for old, current, and future facilities, respectively. An increase in throughput corresponds to increase in methane emissions for the old and current facilities but not the future facility. The number on the box plots shows the mean methane emission.

Table 3.2: Difference in the amount of gas on separators and tanks on the old and current facilities.

Old Facility

Stage 1 Pressure (psig)	Stage 2 Pressure (psig)	Tank Pressure (psig)	Vapor Mass Stage 1 (scf/bbl)	Vapor Mass Stage 2 (scf/bbl)	Vapor Mass Tank (scf/bbl)
250	50	0	41,251	115	96.4

Current Facility

Stage 1 Pressure (psig)	Stage 2 Pressure (psig)	Stage 3 Pressure (psig)	Tank Pressure (psig)	Vapor Mass Stage 1 (scf/bbl)	Vapor Mass Stage 2 (scf/bbl)	Vapor Mass Stage 3 (scf/bbl)	Vapor Mass Tank (scf/bbl)
250	50	2	0	41,014	115	83.9	4.63

MAES models flare and VRU mechanistically, simulating the actual behavior where the amount of emission from the flare and VRU depend on the gas sent to the flare and VRU, which in turn depends on the throughput of the facility. Since the amount of gas from the second stage and the tank sent to the flare for the old site is substantial, the mechanistic emissions from the old site respond more to changes in throughput relative to the current and new facility; see Figure 3.7. For the old facility, percentage of emissions from mechanistic models increased from 29.7 to 60.2 to 79.8 as the throughput increased from 0.5 to 1 to 2. For the current facility, percentage of emissions from mechanistic models increased from 0.311 to 0.555 to 1.09 as the throughput increased from 0.5 to 1 to 2.

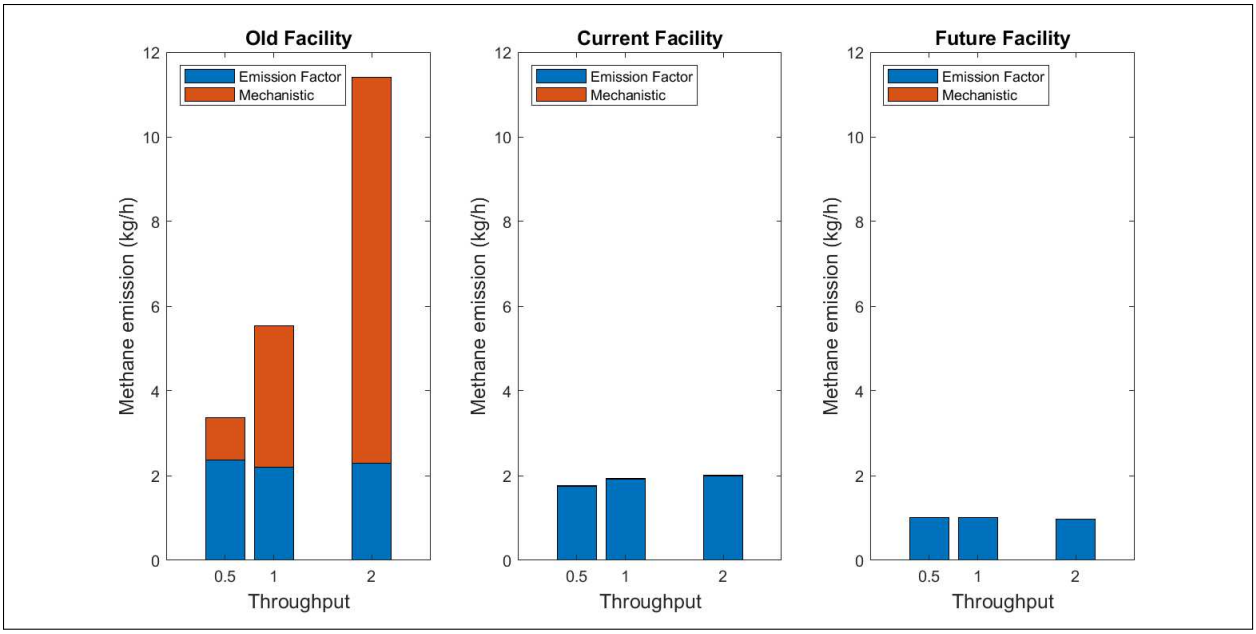

Figure 3.7: From left to right,emission by type of model used to estimate emissions as a function of throughput for old, current, and future facilities, respectively.

This modeling type interests regulators and other stakeholders, as these changes are not readily reflected in traditional inventory methods. For example, the current site has more components than old and future sites. Using the traditional BU approach of activity (component count) multiplied by emission factors, current facilities would be expected to present the highest emissions and the old facility's lowest emissions regardless of the throughput.

Chapter 4

Conclusion

Prototypical sites are useful for basin-level modeling. For example, the DJ basin has over 4,000 sites, and modeling individual sites is cumbersome and costly. Using prototypical sites, all the sites in a basin can be grouped according to their facility design, and the emission behavior and profile can be analyzed. Additionally, using prototypical sites allows detailed modeling of a facility, and as a consequence, issues such as emissions C2/C1 ratio and the impact of facility design can be better understood. Prototypical sites can also be used in methane mitigation by modeling site design changes and analyzing how effective the facility design is in reducing emissions.

The findings of this study showed MAES addressing the three deficiencies in the traditional BU methods, namely the gas composition changes, failure conditions, and variability in facility throughput. MAES could be a tool for regulators and operators to study behaviors of different parameters in estimating emissions. Further, it can be used to make facility design decisions, such as adding a VRU instead of a flare or removing tanks from the facility. MAES could also be used to improve traditional inventory methods and shed some light on reconciling the BU and TD estimates.

TD aerial methods could provide helpful information to populate large emitters models. Plant's study, for instance, provided estimates of the frequency of unlit and malfunctioning flares at sites by using an external survey method [16]. Plant's study used airborne measurements to determine flares destruction efficiencies. The same techniques could be used to determine the frequency and magnitude of failure conditions which could be highly instructive for basin-level inventories. The obtained data could also populate the MAES model to study and understand large emitters models accurately.

Using MAES to simulate emissions comes with several limitations. As of current, MAES does not model working flash; therefore tank emissions are underestimated. Additionally, MAES is not correctly modeling some failure conditions that are key to the production facility emissions, but the

software team is working hard to address the problem. MAES also does not model maintenance emissions, which are a part of reported emissions. Nevertheless, the MAES team is working hard to address these issues and feature more failure models and maintenance emissions to accurately estimate emissions. Future work involves modeling the prototypical site for production facilities and gathering and boosting facilities in the DJ basin with all the critical failure modes.

Bibliography

[1] COGCC Data.

[2] Visualize summary statistics with box plot - MATLAB boxplot.

[3] David T. Allen, Felipe J. Cardoso-Saldaña, and Yosuke Kimura. Variability in Spatially and Temporally Resolved Emissions and Hydrocarbon Source Fingerprints for Oil and Gas Sources in Shale Gas Production Regions. 51(20):12016–12026.

[4] David T. Allen, Felipe J. Cardoso-Saldaña, Yosuke Kimura, Qining Chen, Zhanhong Xiang, Daniel Zimmerle, Clay Bell, Chris Lute, Jerry Duggan, and Matthew Harrison. A Methane Emission Estimation Tool (MEET) for predictions of emissions from upstream oil and gas well sites with fine scale temporal and spatial resolution: Model structure and applications. 829:154277.

[5] David T. Allen, Adam P. Pacsi, David W. Sullivan, Daniel Zavala-Araiza, Matthew Harrison, Kindal Keen, Matthew P. Fraser, A. Daniel Hill, Robert F. Sawyer, and John H. Seinfeld. Methane Emissions from Process Equipment at Natural Gas Production Sites in the United States: Pneumatic Controllers. 49(1):633–640.

[6] Natalie Burclaff. Research Guides: Oil and Gas Industry: A Research Guide: Introduction.

[7] Felipe J. Cardoso-Saldaña, Yosuke Kimura, Peter Stanley, Gary McGaughey, Scott C. Herndon, Joseph R. Roscioli, Tara I. Yacovitch, and David T. Allen. Use of Light Alkane Fingerprints in Attributing Emissions from Oil and Gas Production. 53(9):5483–5492.

[8] Felipe J. Cardoso-Saldaña, Kelly Pierce, Qining Chen, Yosuke Kimura, and David T. Allen. A Searchable Database for Prediction of Emission Compositions from Upstream Oil and Gas Sources. 55(5):3210–3218.

[9] James Crompton and Cheng Siew. The Keys to the Future Oil and Gas Production Facility: The Colorado Story.

[10] Daniel H. Cusworth, Riley M. Duren, Andrew K. Thorpe, Winston Olson-Duvall, Joseph Heckler, John W. Chapman, Michael L. Eastwood, Mark C. Helmlinger, Robert O. Green, Gregory P. Asner, Philip E. Dennison, and Charles E. Miller. Intermittency of Large Methane Emitters in the Permian Basin. 8(7):567–573.

[11] given-i=OAR family=US EPA, given=OAR. Overview of Greenhouse Gases.

[12] given-i=OAR family=US EPA, given=OAR. Understanding Global Warming Potentials.

[13] Christian Frankenberg, Andrew K. Thorpe, David R. Thompson, Glynn Hulley, Eric Adam Kort, Nick Vance, Jakob Borchardt, Thomas Krings, Konstantin Gerilowski, Colm Sweeney, Stephen Conley, Brian D. Bue, Andrew D. Aubrey, Simon Hook, and Robert O. Green. Airborne methane remote measurements reveal heavy-tail flux distribution in Four Corners region. 113(35):9734–9739.

[14] David R. Lyon, Ramón A. Alvarez, Daniel Zavala-Araiza, Adam R. Brandt, Robert B. Jackson, and Steven P. Hamburg. Aerial Surveys of Elevated Hydrocarbon Emissions from Oil and Gas Production Sites. 50(9):4877–4886.

[15] J. Peischl, A. Karion, C. Sweeney, E. A. Kort, M. L. Smith, A. R. Brandt, T. Yeskoo, K. C. Aikin, S. A. Conley, A. Gvakharia, M. Trainer, S. Wolter, and T. B. Ryerson. Quantifying atmospheric methane emissions from oil and natural gas production in the Bakken shale region of North Dakota. 121(10):6101–6111.

[16] Genevieve Plant, Eric A. Kort, Adam R. Brandt, Yuanlei Chen, Graham Fordice, Alan M. Gorchov Negron, Stefan Schwietzke, Mackenzie Smith, and Daniel Zavala-Araiza. Inefficient and unlit natural gas flares both emit large quantities of methane. 377(6614):1566–1571.

[17] Gabrielle Pétron, Anna Karion, Colm Sweeney, Benjamin R. Miller, Stephen A. Montzka, Gregory J. Frost, Michael Trainer, Pieter Tans, Arlyn Andrews, Jonathan Kofler, Detlev Helmig, Douglas Guenther, Ed Dlugokencky, Patricia Lang, Tim Newberger, Sonja Wolter,

Bradley Hall, Paul Novelli, Alan Brewer, Stephen Conley, Mike Hardesty, Robert Banta, Allen White, David Noone, Dan Wolfe, and Russ Schnell. A new look at methane and non-methane hydrocarbon emissions from oil and natural gas operations in the Colorado Denver-Julesburg Basin. 119(11):6836–6852.

[18] Casey Quinn, Daniel Zimmerle, and Daniel B. Olsen. Flare Gas Utilization at Combined Oil-Gas Well Sites. In *ASME 2010 4th International Conference on Energy Sustainability, Volume 1*, pages 279–284. ASMEDC.

[19] Jeffrey S. Rutherford, Evan D. Sherwin, Arvind P. Ravikumar, Garvin A. Heath, Jacob Englander, Daniel Cooley, David Lyon, Mark Omara, Quinn Langfitt, and Adam R. Brandt. Closing the methane gap in US oil and natural gas production emissions inventories. 12(1):4715.

[20] Timothy L. Vaughn, Clay S. Bell, Cody K. Pickering, Stefan Schwietzke, Garvin A. Heath, Gabrielle Pétron, Daniel J. Zimmerle, Russell C. Schnell, and Dag Nummedal. Temporal variability largely explains top-down/bottom-up difference in methane emission estimates from a natural gas production region. 115(46):11712–11717.

[21] Dale Wells. Consequences of the Evolution of Oil and Gas Control and Production Technology in the Denver Ozone Nonattainment Area.

[22] Daniel Zimmerle, Gerald Duggan, Timothy Vaughn, Clay Bell, Christopher Lute, Kristine Bennett, Yosuke Kimura, Felipe J. Cardoso-Saldaña, and David T. Allen. Modeling air emissions from complex facilities at detailed temporal and spatial resolution: The Methane Emission Estimation Tool (MEET). 824:153653.

[23] Daniel Zimmerle, Timothy Vaughn, Ben Luck, Terri Lauderdale, Kindal Keen, Matthew Harrison, Anthony Marchese, Laurie Williams, and David Allen. Methane Emissions from Gathering Compressor Stations in the U.S. 54(12):7552–7561.

Appendix A

Prototypical Sites Description

Although only a few schematics include gas lift compressors, a facility may or may not have a gas lift, and is not a deterministic component to be taken into account when doing the classification. Pressures on the site diagrams are just examples and are not fixed. Also, for all PS, each well is considered to be connected to one HP separator.

- Prototypical Site 1

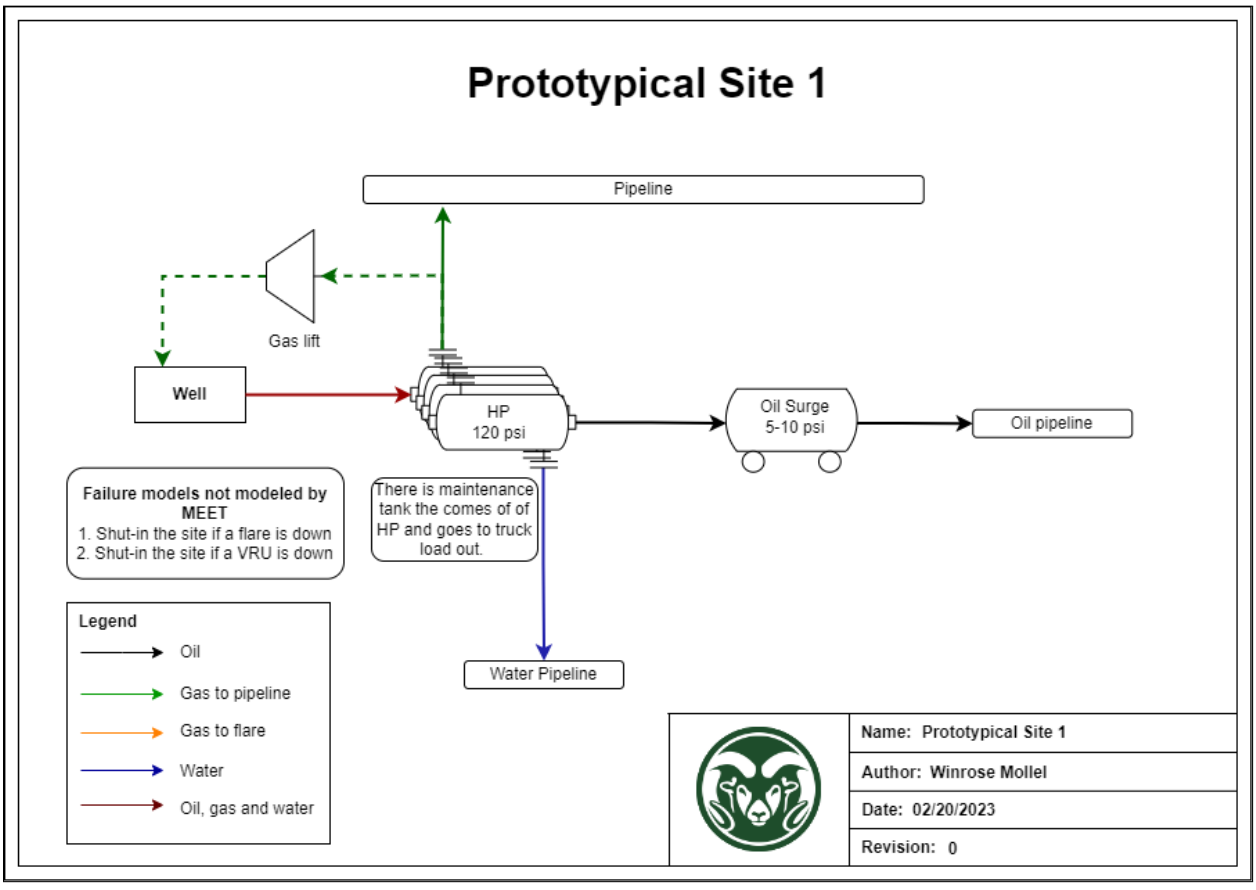

Figure A.1: Prototypical site 1 diagram

A simple well pad with a single stage of separation. The separator is a three-phase HP/direct fire separator. The water from the HP separator goes to the water pipeline, the gas goes to the sales pipeline and the oil goes to an oil surge vessel and then to an oil pipeline.

- Prototypical Site 2

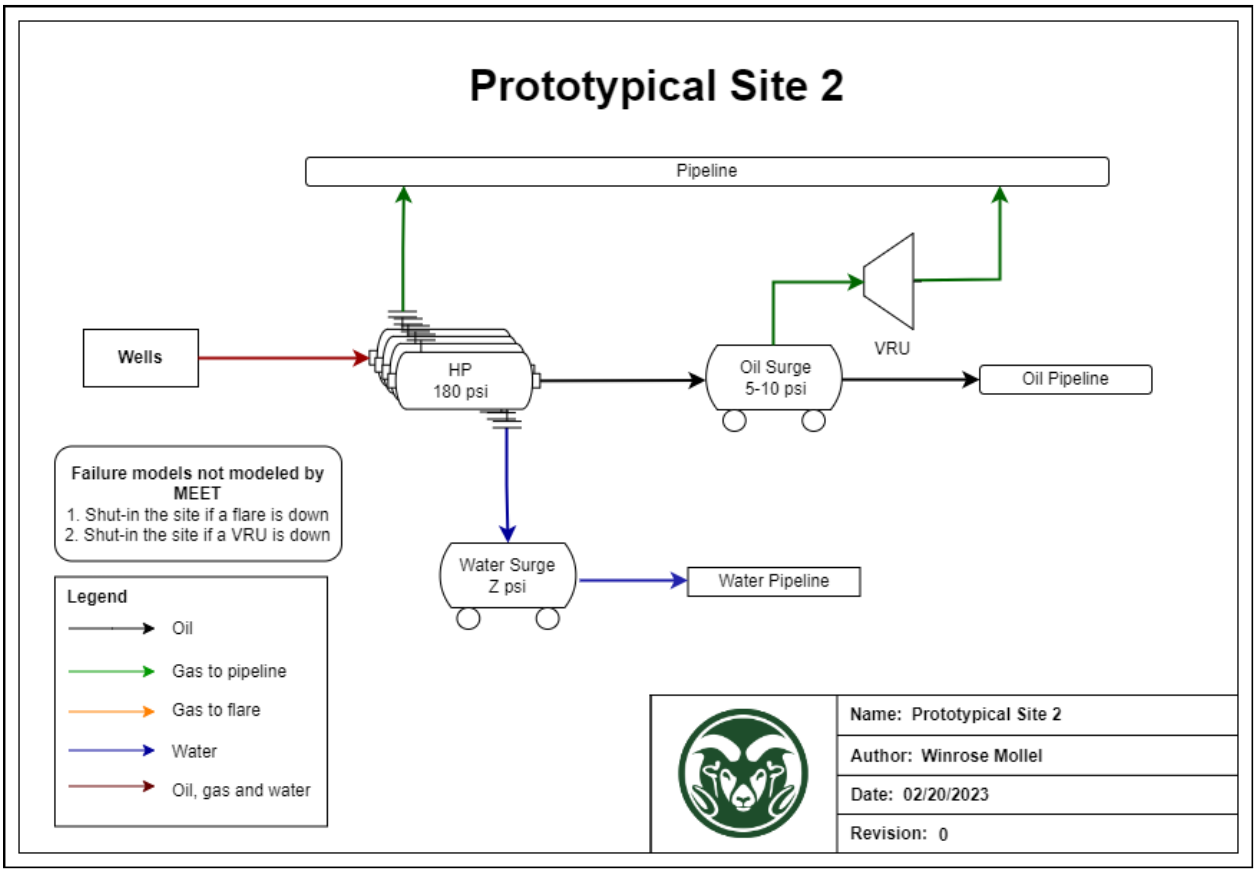

Figure A.2: Prototypical site 2 diagram

A well pad with a single stage of separation. The HP/direct fire separators are three-phase separators. The water from the HP separator goes to the water surge vessel and then to the water pipeline. The gas goes to the gas sales pipeline. Oil goes to an oil surge tank and then to the pipeline. The oil surge vessel is connected to the VRU which compresses the gas to the gas sales line pressure. This facility is tankless.

- Prototypical Site 3

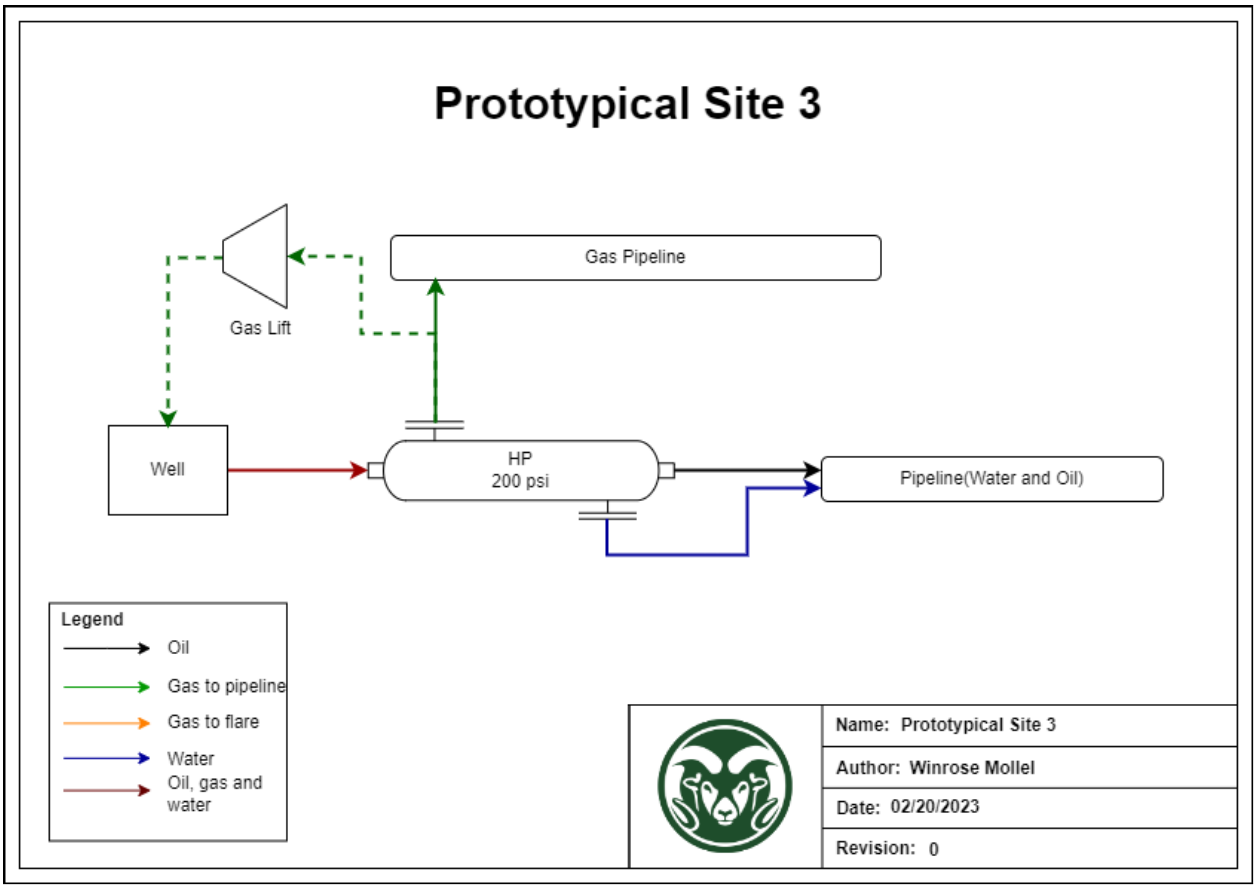

Figure A.3: Prototypical site 3 diagram

A simple well pad with three-phase HP separators. All gas, water, and oil go to the sales line, water, and oil pipeline respectively. This site has a gas lift compressor, and it is a tankless facility.

- Prototypical Site 4

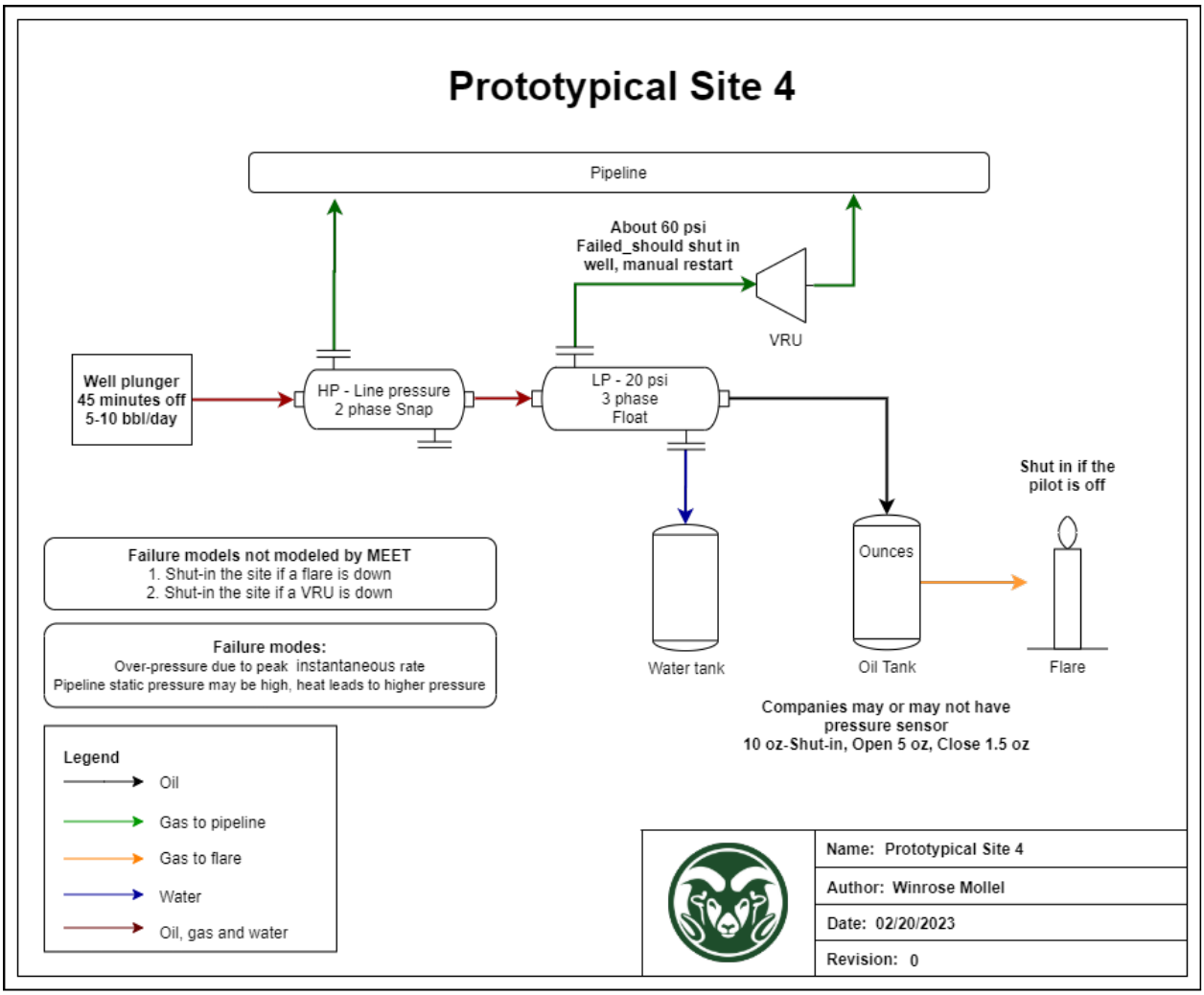

Figure A.4: Prototypical site 4 diagram

A well pad with HLP separators. The gas from the HP side goes to the sales pipeline, and water and oil go to the LP side of the separator. Gas from the LP side goes to a VRU, where it is compressed to sales pipeline pressure. LP side of all separators goes to a single VRU. Both water and oil go to tanks. The oil tanks are connected to the flare.

- Prototypical Site 5

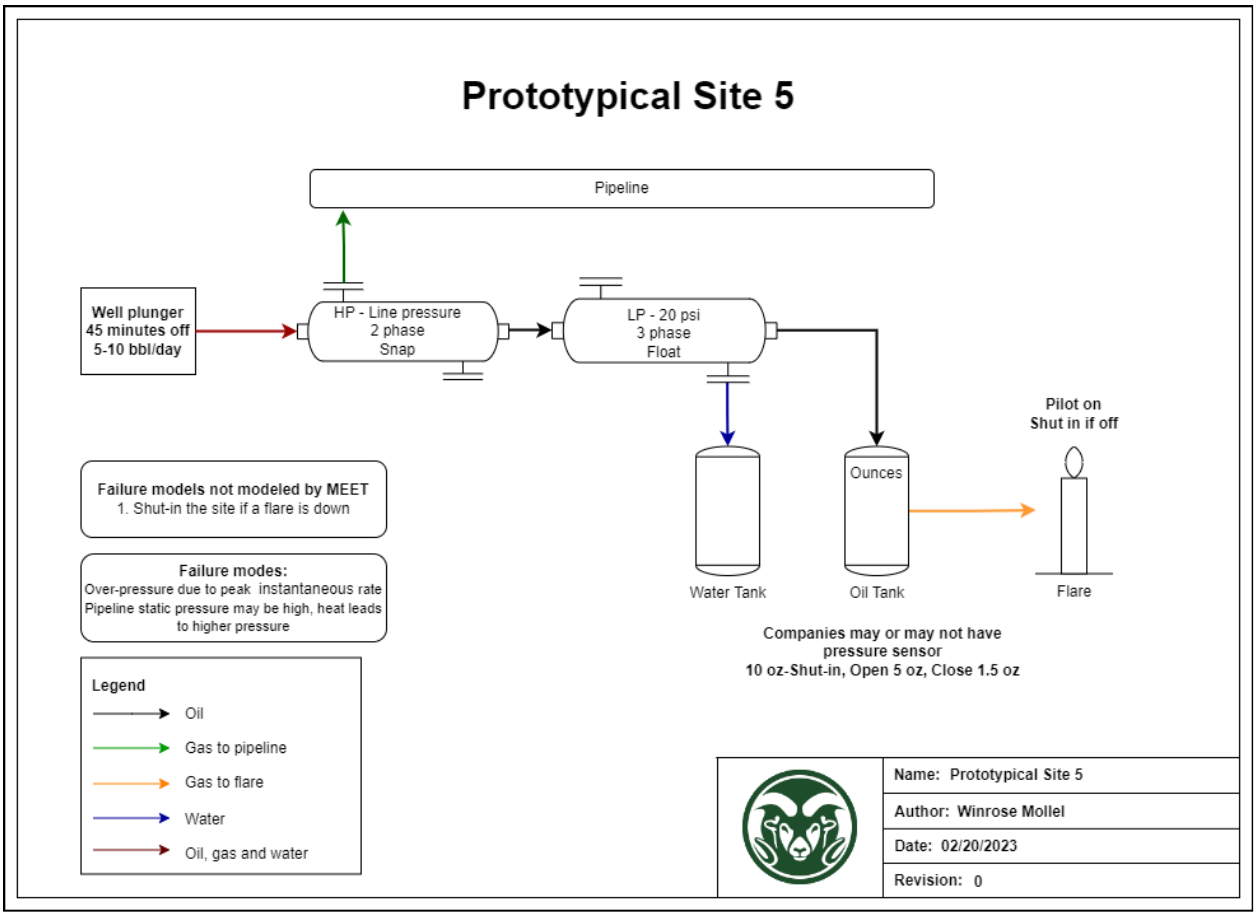

Figure A.5: Prototypical site 5 diagram

A well pad with HLP separators. The gas from the HP side goes to the sales pipeline, and water and oil go to the LP side of the separator. Water from the LP side goes to water tanks, and oil goes to water tanks. The oil tanks are connected to a flare.

- Prototypical Site 6

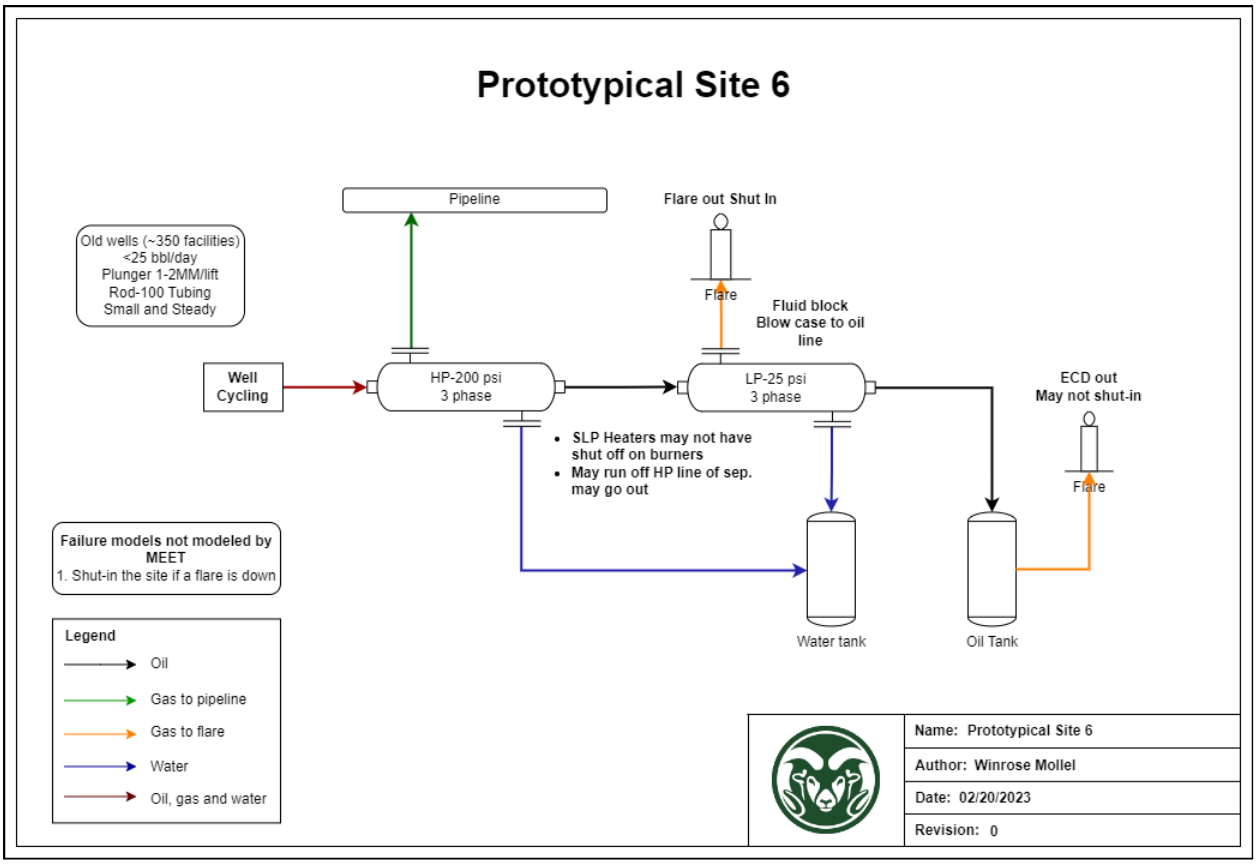

Figure A.6: Prototypical site 6 diagram

A well pad with two stages of separation. The well pad has HP and LP separators, both with three phases of separation. The gas from the HP separators goes to the sales pipeline, the water goes to the water tanks and some to the LP separator, and all oil goes to the LP separator. The gas from the LP separator is flared, water goes to the water tank and oil goes to the oil tank. The oil tank is controlled (Flare).

- Prototypical Site 7

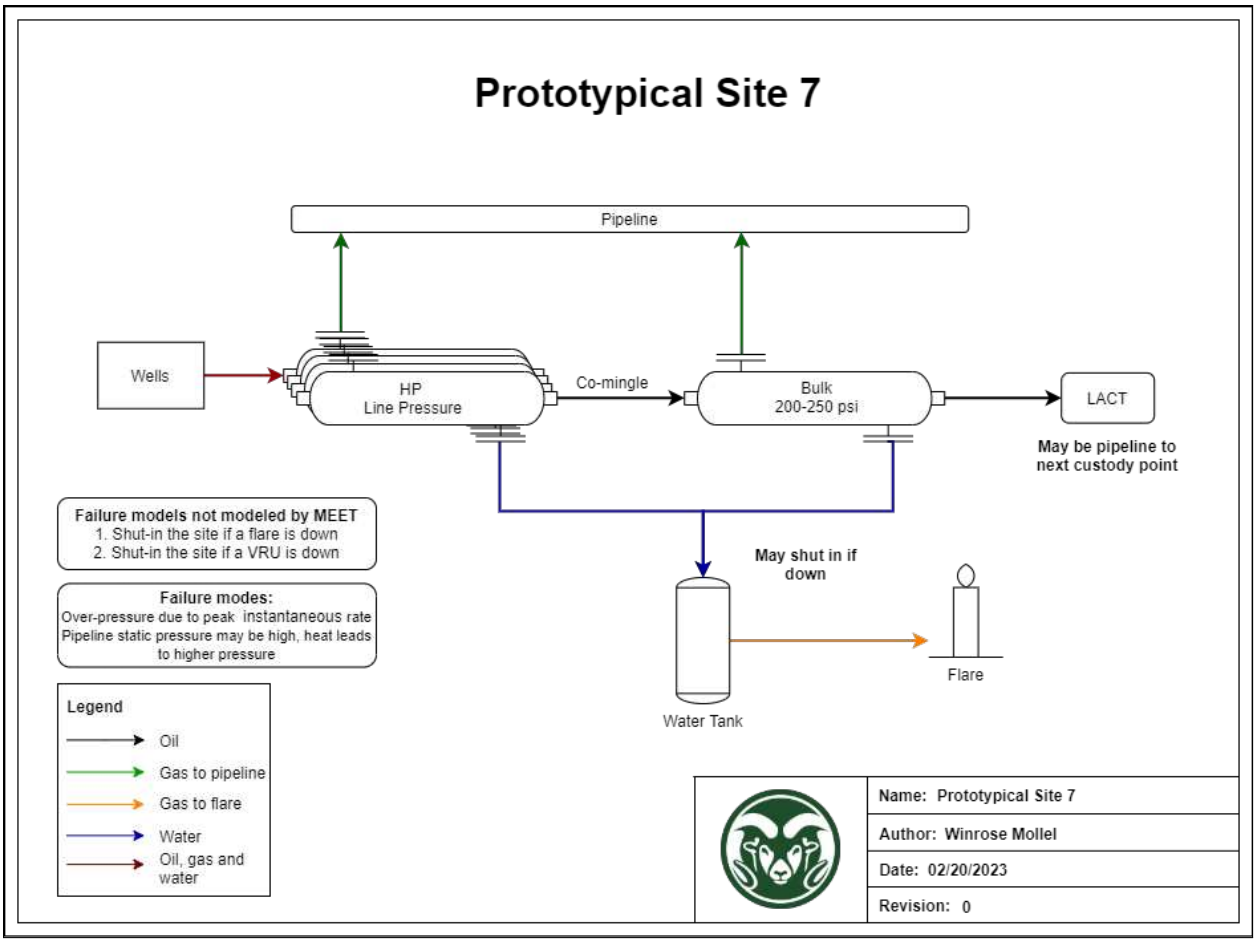

Figure A.7: Prototypical site 7 diagram

A well pad with two stages of separation. HP separators are three-phase separators responsible for the first stage of separation. The gas from the HP separator goes to the sales pipeline, some water goes to the water tanks and all oil goes to the bulk separators. This facility has multiple HP separators connected to a single bulk separator. The oil from the bulk separators goes to the LACT and then to the pipeline. Water goes to the water tank which is controlled. The gas goes to the sales pipeline.

- Prototypical Site 8

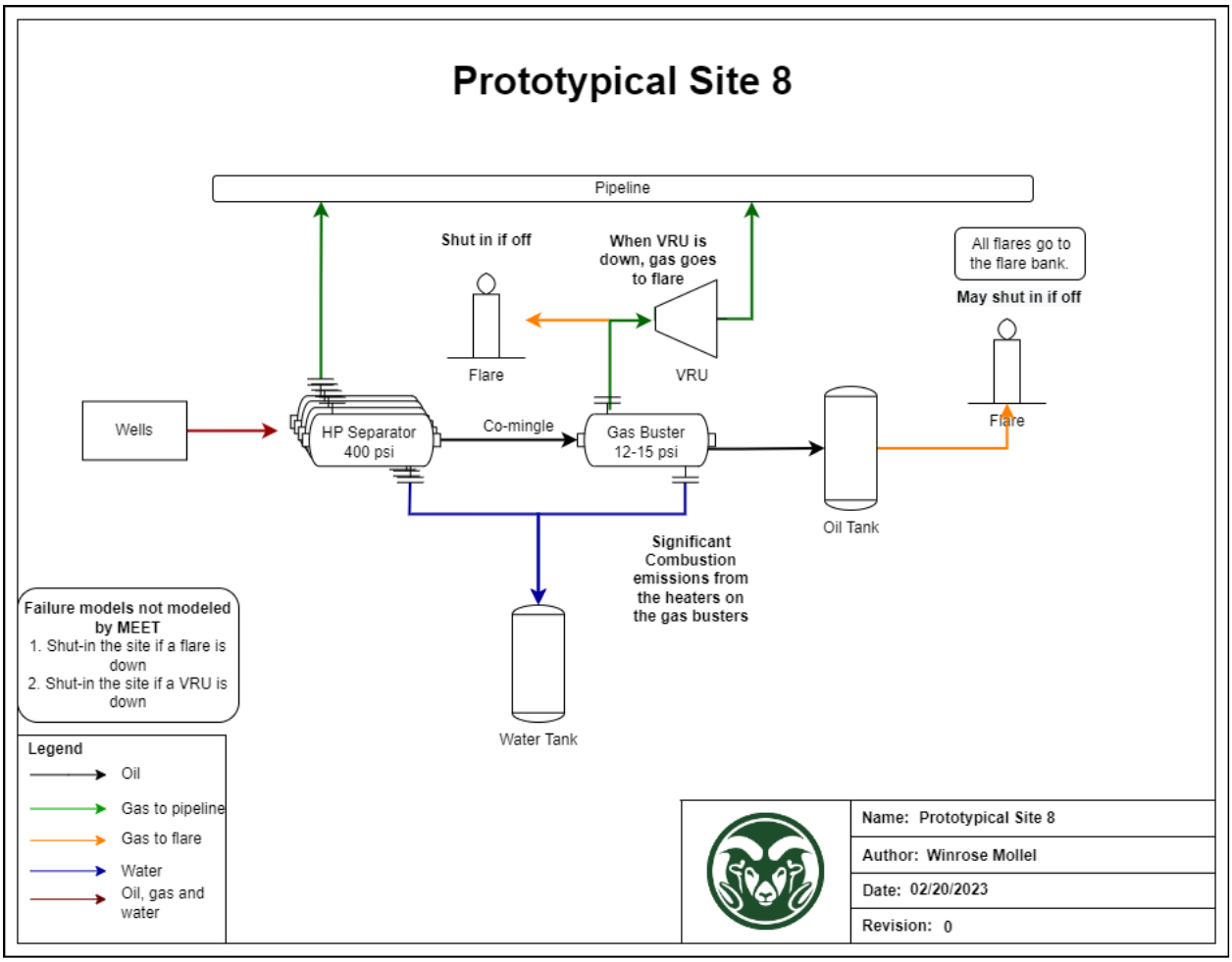

Figure A.8: Prototypical site 8 diagram

A well pad with two stages of separation. HP separators are three-phase separators responsible for the first stage of separation. The gas from the HP separator goes to the sales pipeline, some water goes to water tanks and all oil goes to the gas busters. This facility has multiple HP separators connected to a single gas buster. The oil from the gas buster goes to the oil tanks which are controlled (Flare). Water goes to the water tank. The gas goes to a VRU where it is compressed to sales pipeline pressure. If the VRU goes down all gas will be directed to the flare.

- Prototypical Site 9

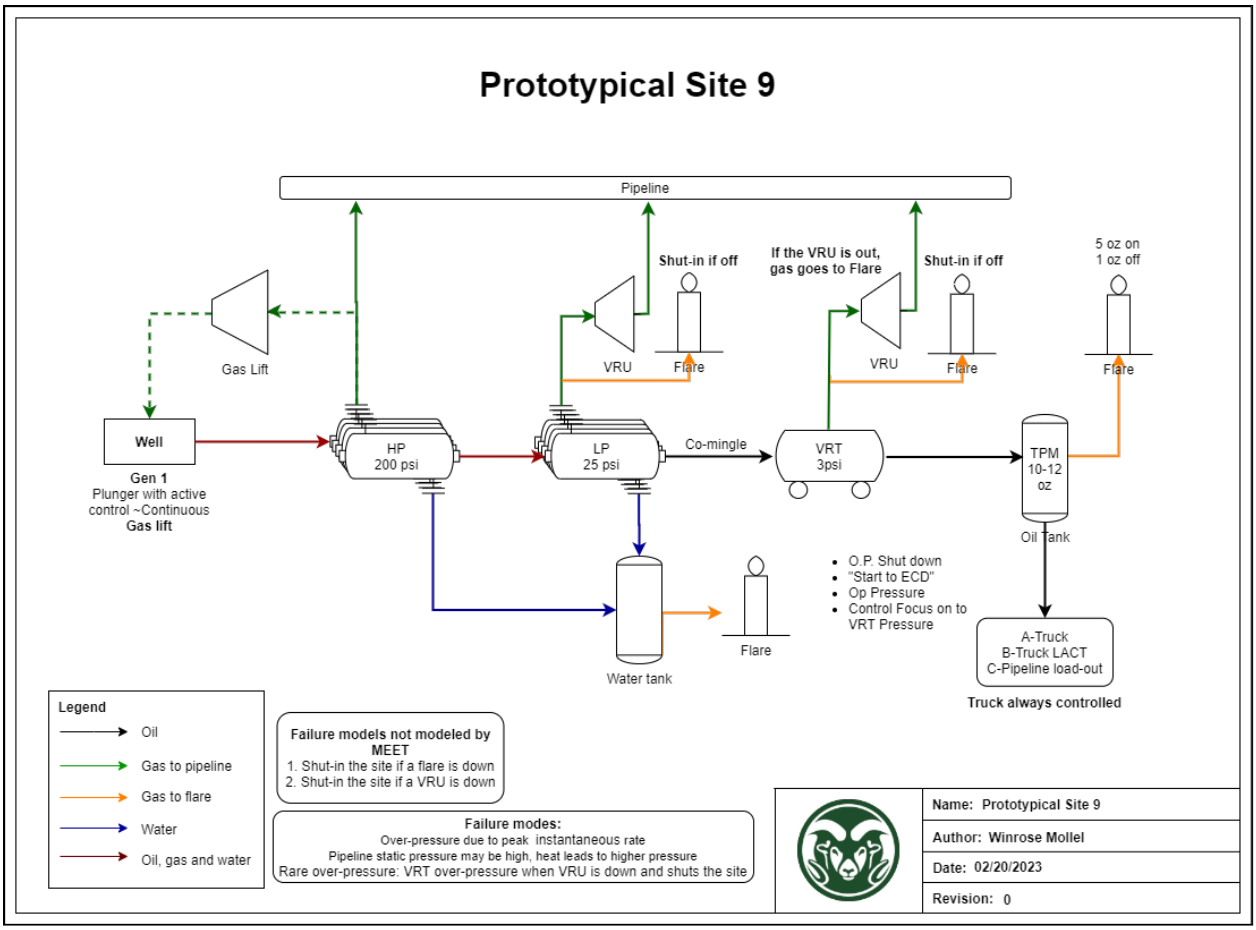

Figure A.9: Prototypical site 9 diagram

A well pad with three stages of separation. The site has HP separators, LP separators, and VRT. Both the HP and LP separators are three phases. The gas from the HP separator goes to the sales pipeline, some water goes to the water tanks and all oil goes to the LP separator. The gas from LP separators is directed to the VRU where it is compressed to the sales pipeline pressure. The oil goes to the VRT, and water goes to the water tanks, which are controlled (Flare). The gas from the VRT goes to the VRU for compression. When the VRUs are out the gas will go to the flare. The oil from the VRT goes to oil tanks which are controlled (Flare). Multiple LP separators go to a single VRT.

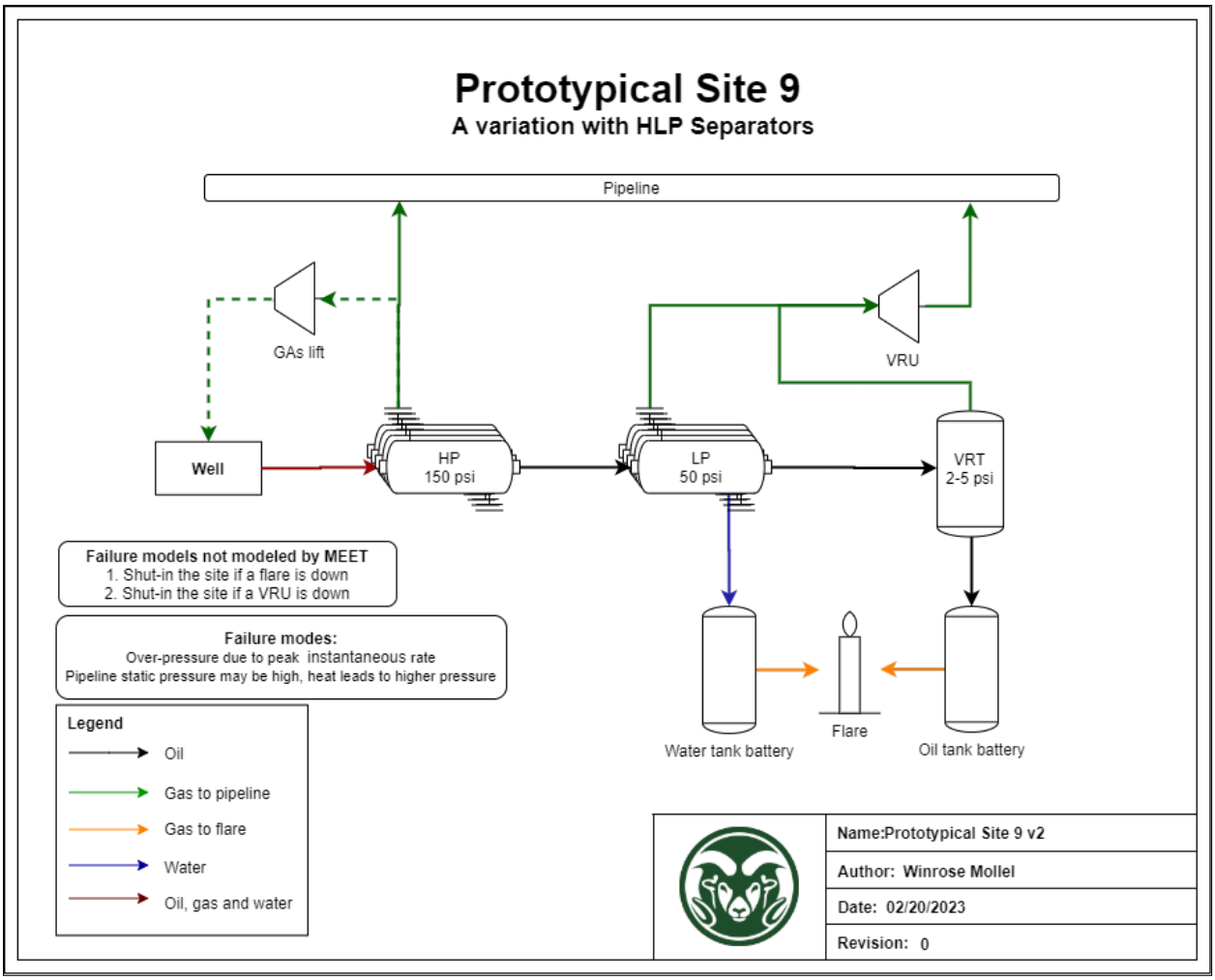

Figure A.10: Prototypical site 9 diagram

This is a variation of site 9 where there is an HLP separator instead of an HP and LP separator. The HP side of the HLP separator has two phases of separation and the LP has three phases. The gas goes to the sales pipeline and water and oil go to the LP side of the HLP separator. Water comes from the LP side of the separator only. Multiple HLP separators are connected to a single VRT.

- Prototypical Site 10

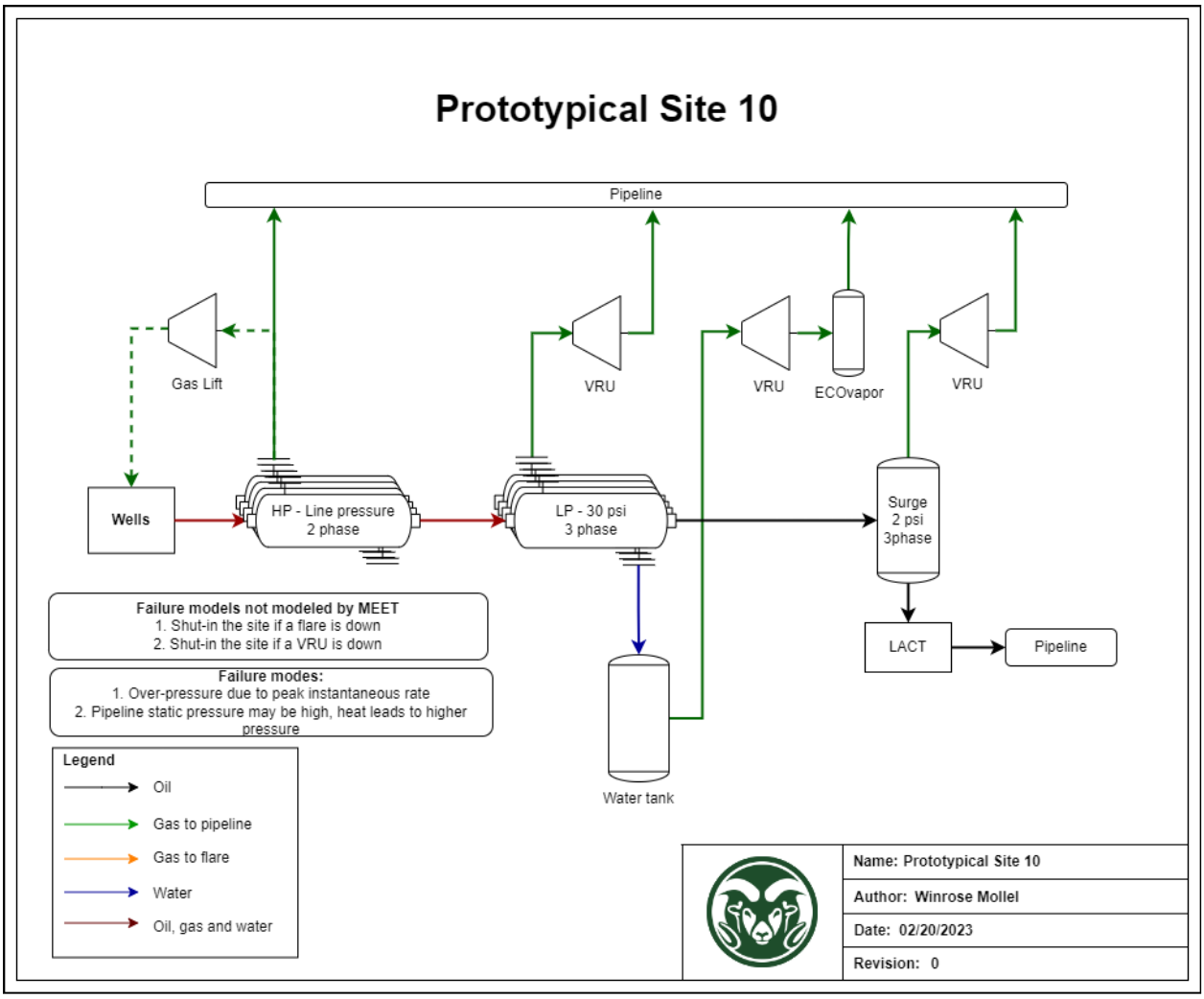

Figure A.11: Prototypical site 10 diagram

A well pad with three stages of separation. The site has HLP separators and a surge vessel. The HP side of the HLP separator has two phases of separation and the LP has three phases. The gas from the HP separator goes to the sales pipeline, and all water and oil go to the LP separator. Gas from LP separators is directed to the VRU where it is compressed to the sales pipeline pressure. The oil goes to the surge vessel and the water goes to the water tanks. The gas from the surge vessel goes to the VRU for compression. When the VRU is out, the gas will go to the flare. The oil from the surge vessel goes to oil tanks. Gas from both water and

oil tanks are directed to a VRU. When the VRUs are down, the flash from the tank will go to the flare. Multiple LP separators go to a single surge vessel.

- Prototypical Site 11

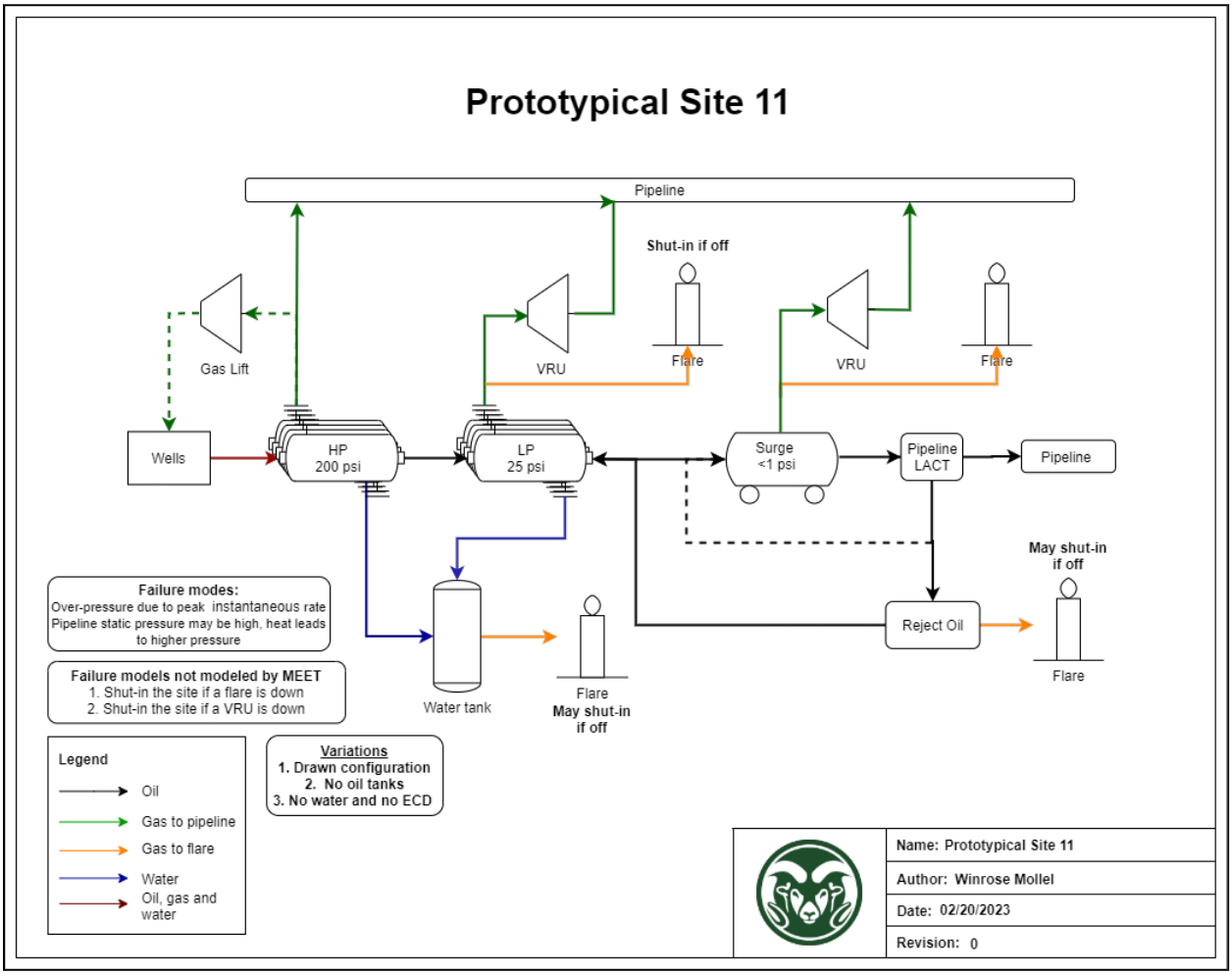

Figure A.12: Prototypical site 11 diagram

A well pad with three stages of separation. The site has HLP separators, LP separators, and a surge vessel. Both HP and LP separators are three phases. The gas from the HP separator goes to the sales pipeline, some water, and all oil goes to the LP separator, and the remaining water goes to the water tank. The gas from LP separators is directed to the VRU where it is compressed to the sales pipeline pressure. The oil goes to the surge vessel and water goes

to the water tanks. The gas from the surge vessel goes to the VRU for compression. When the VRUs are out, the gas will go to the flare. The oil from the surge vessel goes to LACT and then to the oil pipeline. Sometimes the oil from the LACT goes to a reject oil tank. The reject oil tank is then fed back to the HP separator. Multiple LP separators go to a single surge vessel. The water tanks are controlled.

- Prototypical Site 12

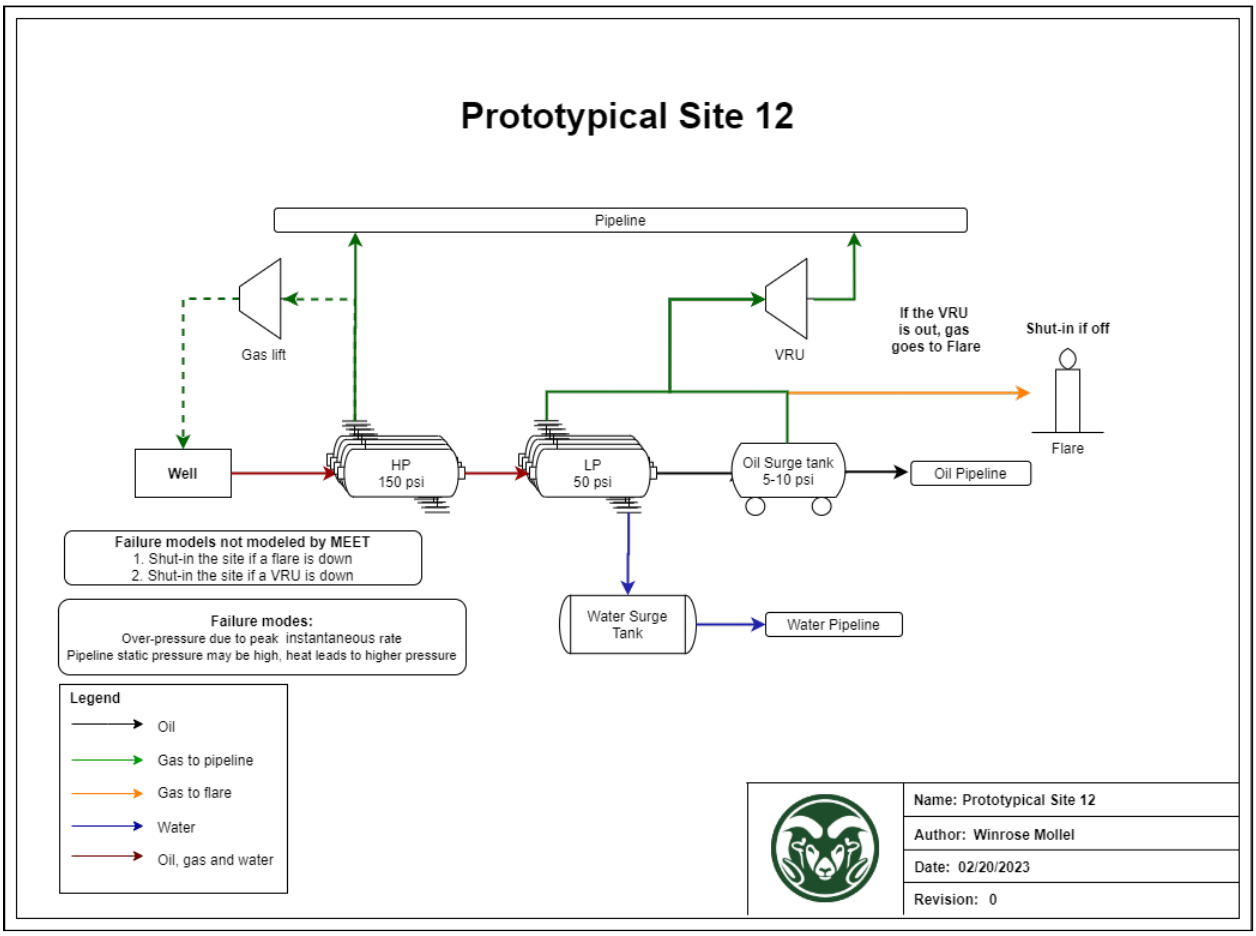

Figure A.13: Prototypical site 12 diagram

A well pad with three stages of separation. The site has HLP separators and a surge vessel. The HP side of the HP separator has two phases of separation and the LP has three phases. The gas from the HP separator goes to the sales pipeline, and all water and all oil go to the

LP separator. The gas from LP separators is directed to the VRU where it is compressed to the sales pipeline pressure. The oil goes to the surge vessel and water goes to the water pipeline. The gas from the surge vessel goes to the VRU for compression. When the VRUs are out the gas will go to the flare. The oil from the surge vessel goes to the oil pipeline. Multiple LP separators go to a single surge vessel. This facility is tankless.

- Prototypical Site 13

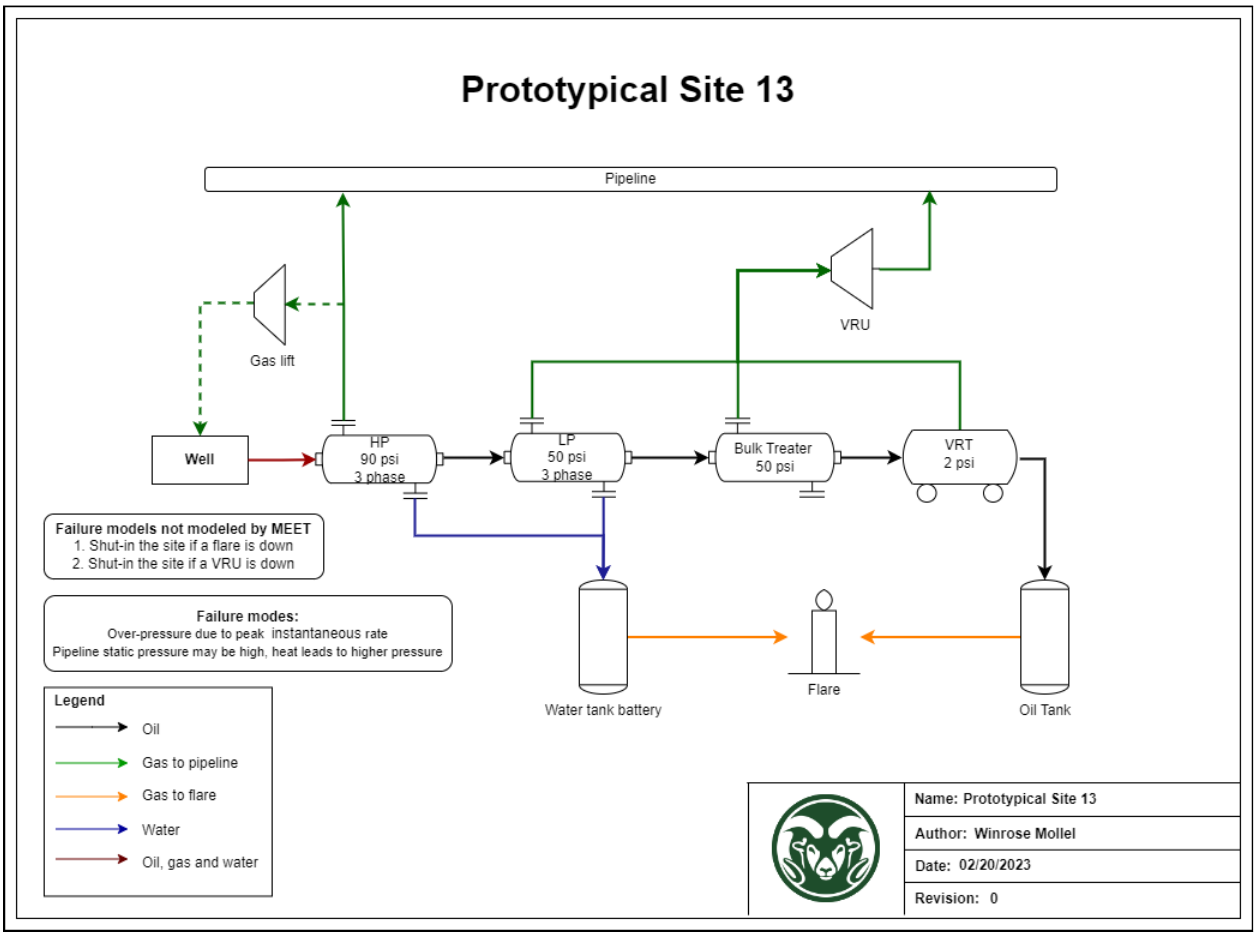

Figure A.14: Prototypical site 13 diagram

A well pad with four stages of separation. The site has HP separators, LP separators, a bulk treater, and a VRT. Both HP and LP separators are three-phase separators. The gas from the HP separator goes to the sales pipeline, some water, and all oil goes to the LP separator, and

the remaining water goes to the water tank. The gas from LP separators is directed to the VRU where it is compressed to the sales pipeline pressure. The oil goes to the bulk treater then to a VRT and water goes to the water tanks. The gas from both the bulk treater and VRT goes to the VRT for compression. The oil from the VRT goes to oil tanks. Multiple LP separators go to a single bulk treater. Both oil and water tanks are controlled.

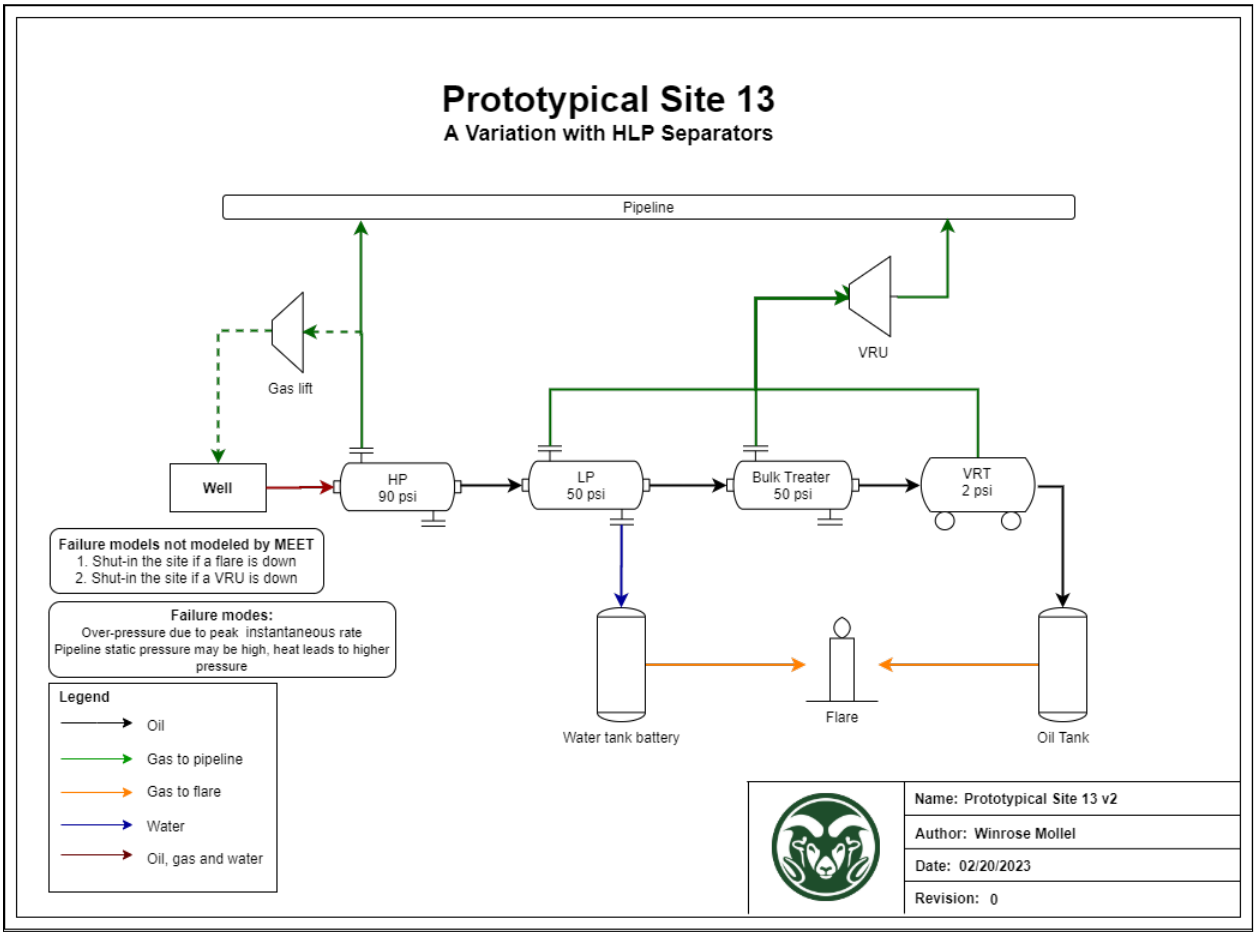

Figure A.15: Prototypical site 13 variation diagram

This is a variation of site 13 with HLP separators instead of HP and LP separators.

Appendix B

Gas compositions

The gas composition depends on wellhead composition, pressure at each stage of separation, and process temperature [8]. The gas composition file includes the composition at each stage of separation, tanks, and a facility level. The wellhead composition used is shown in Table B.1.

Table B.1: Wellhead composition.

Specie	CO2	N2	H2S	C1	C2	C3	iC4	C4	iC5	C5	C6	C7plus
(%)	1.91	5.67	0.02	68.98	11.65	5.69	0.82	1.92	0.44	0.42	0.51	1.97

[1] Species by mass fraction

[2] CO2-Carbon dioxide, N2-Nitrogen, H2S-Hydrogen Sulphide, C1-Methane, C2-Ethane, C3-Propane, iC4-Isobutane, C4-Butane, iC5-Isopentane, C5-Pentane, C6-Hexane, C7plus-Higher HCs

The main assumptions for the gas composition generations are, total gas is the sum of the gas streams leaving each flashing stage and the amount of hydrocarbons dissolved in water is minimal since they are not miscible. Therefore, water flash is calculated at the tanks only. To generate a gas composition file the following are the main requirements: Gas to oil ratio(GOR), API gravity, process temperature, and pressure at each stage of separation [8].

The gas composition file is generated in two steps, generation of the wellhead compositions and running the wellhead composition through each stage of separation. (Pro-max can be used to generate the gas composition instead)

The wellhead composition was determined by using a database of possible wellhead compositions in different basins in the US. The gas composition at each stage of separation was calculated using an existing code. The code uses the wellhead composition, separation pressures, and temperature to calculate the molar fraction of species using thermodynamics relations. Molar fractions for each stage of separations are calculated using the Behrens and Sandler lumping scheme and Peng and Robinson equation of state. Species with zero molar fraction are removed. The phase

equilibria calculations of the water are independent of the hydrocarbon ones. A mole of a given mixture of hydrocarbons and inert (N2, H2S, and CO2), but not water, enter the first stage separator. Then the phase equilibria are calculated with the assumption that the molar flow rate of the species entering the first stage separator is one mole. Then the Peng-Robinson Equation of State (PR-EOS) indicates the number of moles that go to the gas phase and the number of moles to the liquid hydrocarbon phase, and the compositions of both of those streams, solving the system. As you go to other separators the same process is repeated but now the molar flow rate of the stream entering the "nth" stage separator or tank at atmospheric pressure is dependent on the previous one. Then the composition of the produced gas in the first stage separator is used to calculate the molar fraction of hydrocarbons in the water phase. In the first stage separator, the water stream is separated and goes to the water tanks, then in the "nth" stage separator there is no more water. The water flashing emissions occur in the water tank.

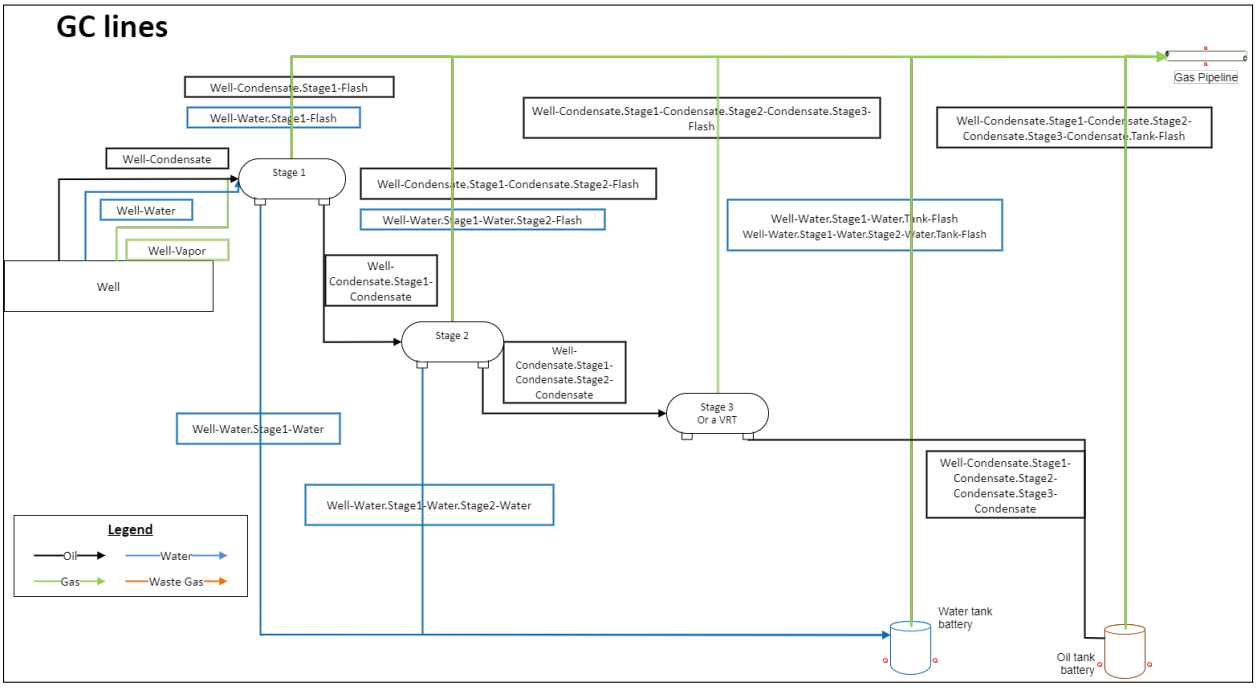

Figure B.1: Gas Composition lines representing the gas composition generated for each major equipment

C2C1 ratio changes with pressure ratio changes

Pressure ratio variations result in the C2/C1 ratio changes. Primarily because methane is a lighter molecule than ethane, therefore, a decrease in pressure results in more methane being flashed than ethane. Additionally, methane is the main component of natural gas, subsequently more methane is flashed at any pressure than ethane. For this study, the wellhead composition and the process temperature remained constant while the pressure varied. The wellhead composition used is shown in Table B.1. Gas composition was calculated for all pressure variations. The pressure of the first stage of separation remained constant at 250 psig, the pressure of the second stage of separation varied between 240 psig and 50 psig, and the pressure of the third stage of separation varied between 15 psig and 2 psig.

Table B.2: The C2/C1 ratio increases with increase in pressure ratio

Stage 1 Pressure (psig)	Stage 2 Pressure (psig)	Stage 3 Pressure (psig)	Pressure Ratio (psia/psia)	Units	Methane	Ethane	C2/C1
250	240	15	1.0393	Kg/bbl	0.0489	0.0159	0.3241
250	200	15	1.2331	Kg/bbl	0.2539	0.0947	0.3730
250	150	5	1.6079	Kg/bbl	0.5203	0.2428	0.4667
250	100	2	2.3100	Kg/bbl	0.7759	0.4843	0.6241

Appendix C

Number of wells-Sensitivity Study

A sensitivity study to examine the effect of increasing the number of wells for facilities with increasing complexity was done. An increasing number of wells leads to an increase in the facility throughput. The facilities were classified into three categories: simple, medium, and complex according to their complexity. The simple facility had only one well. The number of wells was then increased to ten wells with an increment of 1 well. The medium complexity facility had five wells, the number of wells was increased to ten wells and decreased to one well at an increment of one well respectively. The complex facility had eleven wells, the number of wells was decreased to six and increased to sixteen by increment of one well respectively.

- Simple Facility

  As you increase the number of wells, the total methane emissions from the site also increase. Increasing nine wells led to a 340 percent increase in methane emissions. Emissions were divided into four categories to see how they vary with the number of wells. These categories include combusted, fugitive, pneumatic venting, and large fugitive. The combusted category includes all combustion emissions from the compressor exhaust and the flare. Fugitive is the sum of all component leaks. Large fugitives included large tank emissions. Pneumatic venting is the emissions from pneumatic controllers present in the facility. The slope for each category was calculated. Combusted, fugitive and pneumatic venting had a good fit with R squared value of greater than 0.8 and a slope of 0.008, 0.065, and 0.50 kg/h of methane per well respectively. The fraction of slope for combusted, fugitive, and pneumatic venting was 0.014, 0.114, and 0.872 respectively.

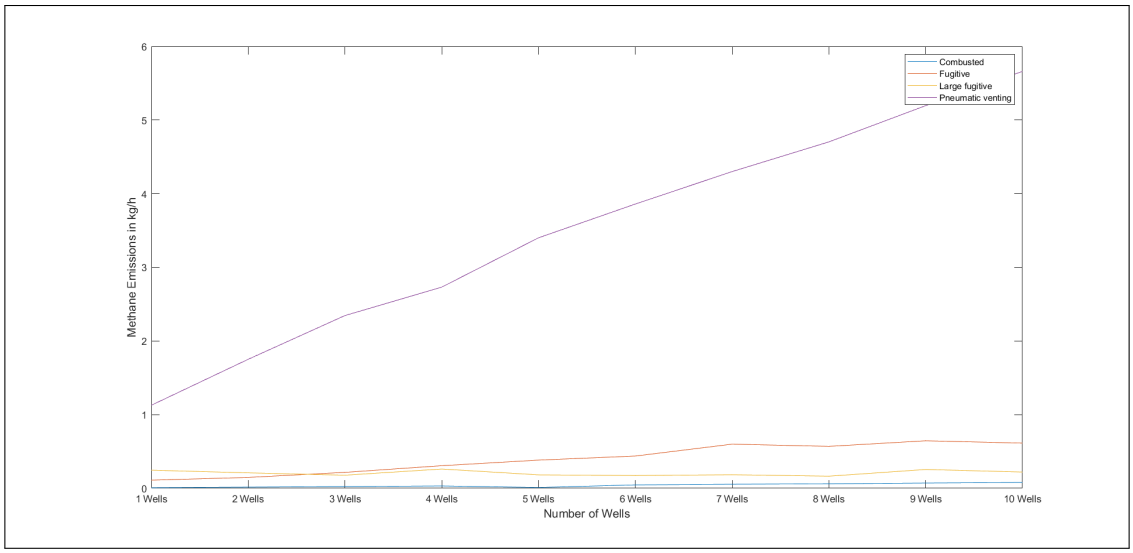

Figure C.1: The effect of increasing the number of wells in a simple facility.

- Medium Facility

  Increasing five wells led to a 39 percent increase in methane emissions while decreasing four wells led to a 42 percent decrease in methane emissions. Medium facility total emissions were divided into six categories which were combusted, event, fugitive, large fugitive, large vent, and pneumatic venting. Events represent compressor blowdowns and the large vent is for rod-packing venting from the compressors. The R squared value for the event, large vent, and large the fugitive was less than 0.8, therefore these categories were considered a bad fit. Combusted, fugitive and pneumatic venting has a good fit with a slope of 0.004,0.062, and 0.032 kg/h of methane per well. The faction of slope for combusted, fugitive, and pneumatic venting was 0.039,0.633, and 0.329 respectively.

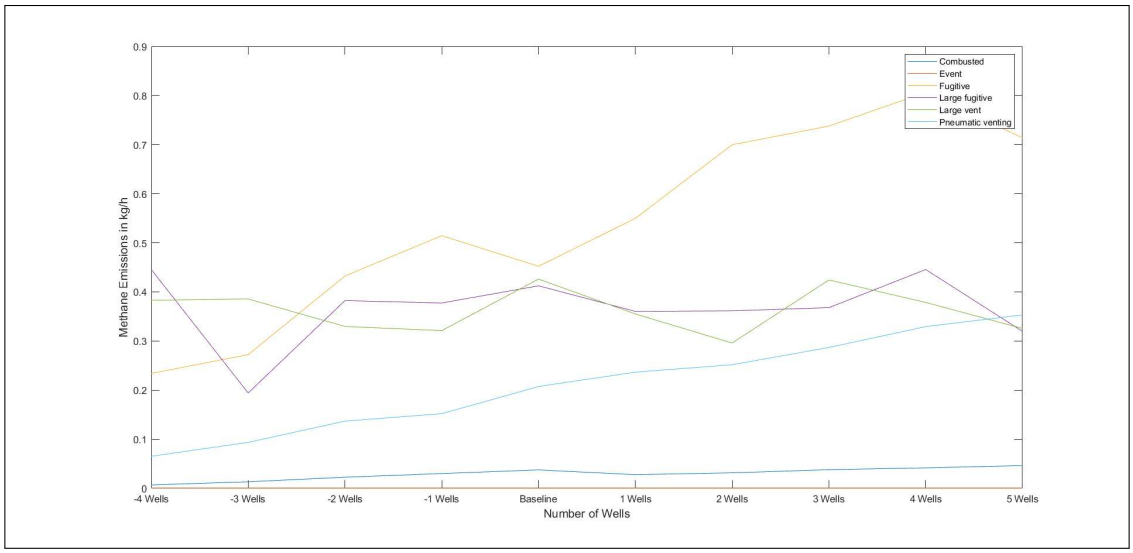

Figure C.2: The effect of increasing the number of wells in a medium facility.

- Complex facility

  Increasing five wells led to a 36 percent increase in methane emissions while decreasing five wells led to a 36 percent decrease in methane emissions. Complex facility total emissions were divided into six categories which were combusted, event, fugitive, large fugitive, large vent, and pneumatic venting. For medium facility, event, large fugitive, and large vent has a bad fit. Combusted, fugitive, and pneumatic venting slope was 0.004, 0.011, and 0.508 kg/h of methane per well. The fraction of slope for combusted, fugitive, and pneumatic venting was 0.006, 0.129, and 0.865 respectively.

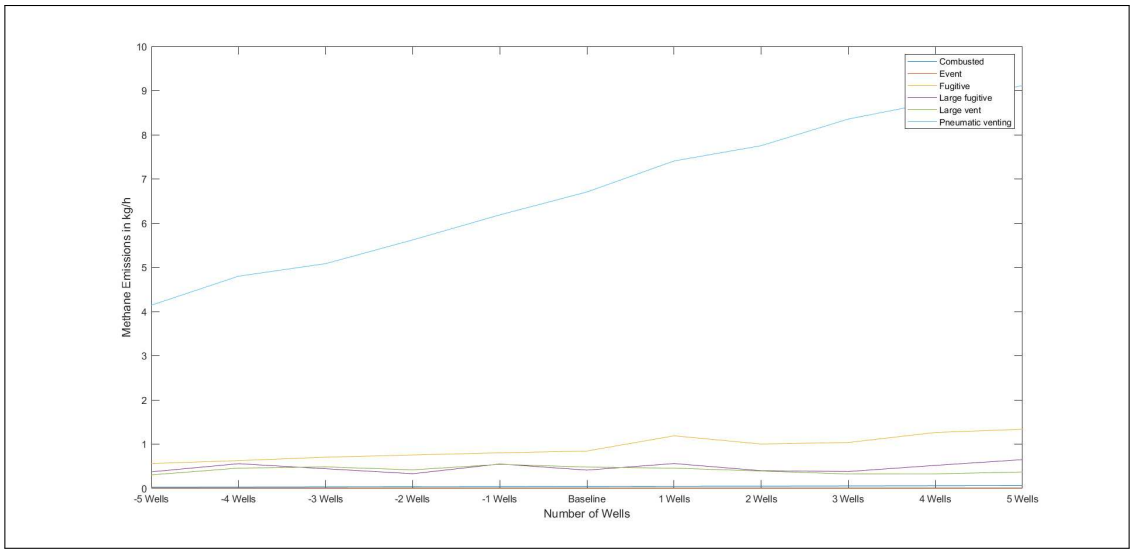

Figure C.3: The effect of increasing the number of wells in a complex facility.

Fugitive show a linear relationship with wells because the number of wells affects the number of components in the wellpad. Pneumatic also depends on components on the well pad therefore increasing number of wells led to increasing number of pneumatic thus increase in methane emissions. Combustion emissions depend on how much gas is sent to the flare. Flare uses mechanistic models and depends on fluids flow therefore, increasing number of wells increases facility throughput and thus increase in amount of gas sent to the flare. For all facilities, increase number of wells led to an increase in methane emissions for combusted, fugitive and pneumatic venting respectively. For modeling purposes, facilities with the same configuration but different number of wells should be modeled separately.

Appendix D

Markov Transition Matrix

A Markov transition matrix is a square matrix that represents the probability of changing states in a dynamic system. In each row are the probabilities of moving from the state represented by that row to the other states. Each row of a Markov transition matrix adds to unity. Markov a matrix is denoted as Q(x' | x) meaning Q is a matrix, x is the existing state, x' is a possible future state, and for any x and x' in the model, the probability of going to x' given that the existing state is x, is in Q.

Markov transition Matrix was used to determine the time in each state of a flare. A flare has three states: Operating, malfunctioning, and Unlit. To set the failure rates observed in the field, we assume that the flare will operate normally 100% of the time, malfunction 85% of the time, and be unlit 15% of the time. The operating time varies from 30 to 90 days in length and then transitions into a malfunction state – either poor combustion (85% of transitions) or unlit (15% of transitions). Time in malfunction is 1 to 7 days and time in unlit is 1 to 2 days.

Flare Transition Matrix $\begin{bmatrix} 0.00 & 0.85 & 0.15 \\ 1.00 & 0.00 & 0.00 \\ 1.00 & 0.00 & 0.00 \end{bmatrix}$

Time in each state $\begin{bmatrix} 60 \\ 7 \\ 2 \end{bmatrix} \begin{bmatrix} Operating \\ Malfuctioning \\ Unlit \end{bmatrix}$

Days in each state $\begin{bmatrix} 30 \\ 3 \\ 0.15 \end{bmatrix}$

Fraction of time in each state $\begin{bmatrix} 0.906 \\ 0.090 \\ 0.005 \end{bmatrix}$